Psychophysiology, 44 (2007), 949–967. Blackwell Publishing Inc. Printed in the USA.

DOI: 10.1111/j.1469-8986.2007.00562.x

Reference-independent ERP old/new effects of auditory and visual word recognition memory: Joint extraction of stimulus- and response-locked neuronal generator patterns

JÜRGEN KAYSER,[a,b] CRAIG E. TENKE,[a,b] NATHAN A. GATES,[a] AND GERARD E. BRUDER[a,b]

[a]Division of Cognitive Neuroscience, New York State Psychiatric Institute, New York, New York, USA
[b]Department of Psychiatry, Columbia University College of Physicians & Surgeons, New York, New York, USA

Abstract

To clarify polarity, topography, and time course of recognition memory ERP old/new effects during matched visual and auditory continuous word recognition tasks, unrestricted temporal PCA jointly analyzed stimulus- and response-locked, reference-free current source densities (31-channel, $N = 40$). Randomization tests provided unbiased statistics for complete factor topographies. Old/new left parietal source effects were complemented by lateral frontocentral sink effects in both modalities, overlapping modality-specific P3 sources 160 ms preresponse. A mid-frontal sink 45 ms postresponse terminated the frontoparietal generator pattern, showed old/new effects consistent with bilateral activation of anterior cingulate and SMA, and preceded similar activity extending posteriorly along the longitudinal fissure. These methods separated old/new stimulus source (preresponse) and response sink (postresponse) effects from motor and modality-specific ERPs.

Descriptors: Recognition memory, Event-related potential (ERP), Current source density (CSD), Principal components analysis (PCA), Stimulus- and response-locked, Visual and auditory modality

Neuroimaging methods do not generally provide direct, real-time measures of brain activity associated with successive stages of information processing. By virtue of its temporal and spatial (i.e., topographic) signal characteristics, the widely used event-related potential (ERP) technique has significantly shaped the understanding of many neurocognitive processes, including mnemonic functions (e.g., Allan, Wilding, & Rugg, 1998; Friedman, 2000). One of the most robust findings in ERP memory research, a more positive-going potential for correctly recognized old than new items, is considered an electrophysiological correlate of explicit episodic memory-retrieval processes (for reviews, see, e.g., Friedman & Johnson, 2000; Johnson, 1995; Mecklinger, 2000; Wilding, 2000). This so-called old/new effect begins around 300 ms after stimulus onset, extends for several hundred milliseconds, shows a left parietal maximum, and can be observed to a different degree for a great variety of stimulus categories (words, pictures, faces, etc.), memory paradigms (study–test, continuous recognition), processing modalities (visual, auditory), and populations (young vs. old, schizophrenic patients vs. healthy adults, etc.; e.g., Friedman, 1990a, 1990b; Guillem et al., 2001; Kayser et al., 1999; Kayser, Fong, Tenke, & Bruder, 2003; Paller & Kutas, 1992; Rugg, 1985, 1987; Wilding, Doyle, & Rugg, 1995).

The old/new effect, however, is not a single, unitary phenomenon in ERP studies of episodic memory, but includes several subcomponents that can also be associated with specific functions of memory retrieval (e.g., Johansson & Mecklinger, 2003). Dual-process theories assume that recollection and familiarity are two distinct retrieval processes underlying recognition memory (e.g., Yonelinas, 2001). Whereas conscious recollection has been linked to the left parietal old/new effect, a somewhat earlier mid-frontal old/new effect, peaking around 400 ms, has been connected with item familiarity (e.g., Curran, 1999; Curran & Cleary, 2003). To the best of our knowledge, this mid-frontal episodic memory effect has only been reported for visual but not auditory ERPs. These positive old/new effects overlap either a positive component (parietal P3 or P600) or a negative

The National Institute of Mental Health (NIMH) supported this research through grants MH50715 and MH066597. We thank Charles L. Brown, III, for developing a fine software for waveform plotting. Preliminary analyses of these data were presented at the 42nd Annual Meeting of the Society for Psychophysiological Research (SPR), October 2–6, 2002, Washington, DC, and the International Congress of Biological Psychiatry, Sydney, Australia, February 9–13, 2004. We are grateful for several helpful comments received during the review process.

Address reprint requests to: Jürgen Kayser, New York State Psychiatric Institute, Division of Cognitive Neuroscience, Unit 50, 1051 Riverside Drive, New York, NY 10032, USA. E-mail: kayserj@pi.cpmc.columbia.edu

component (mid-frontal FN400). In contrast, a negative-going old/new effect manifests as a posterior slow wave at or around the time of the subjects' response (e.g., Cycowicz, Friedman, & Snodgrass, 2001; Kayser et al., 1999, 2003; Nessler & Mecklinger, 2003). Lacking a compelling functional explanation, this late negative-going episodic memory effect has attracted less attention until recently, when it has tentatively been linked to a response-related error negativity (ERN/Ne) reflecting action monitoring and/or reevaluation of item-specific attributes during retrieval (Friedman, Cycowicz, & Bersick, 2005; Johansson & Mecklinger, 2003). These authors have suggested that the functional role of this late episodic memory effect could be clarified by directly comparing this effect for different stimulus modalities or by aligning ERPs to response onset. The current study incorporates both of these suggestions by building on our previous report that used matched auditory and visual continuous recognition memory tasks (Kayser et al., 2003), but did not specifically address these more recent hypotheses regarding the meaning of the late episodic memory effect.

Lingering Issues: ERP Recording Reference and Component Definition

Two problems that have plagued ERP research are the dependency of surface potentials on a reference location (e.g., linked mastoids, nose, average) and the definition and measurement of appropriate ERP components (e.g., specific time windows for peak or integral amplitudes), which crucially affect component interpretation (e.g., polarity, topography, generator) and statistical analysis (e.g., Kayser & Tenke, 2003, 2005; Nunez & Srinivasan, 2006; Tenke & Kayser, 2005). To the extent that the reference region is affected by the experimental manipulation, regional condition effects are altered, that is, introduced (amplified) or removed (reduced), at other regions following volume-conduction principles of simple summation by choice of reference. Although it is common knowledge among ERP researchers that no recording site placed anywhere on the human body can be considered electrically inactive (e.g., sternum, neck, mastoid, nose, ear lobe, vertex, average,[1] etc.) and any site will be differentially affected by a given combination of neuronal generators through volume-conducted activity (e.g., Nunez, 1981; Nunez & Westdorp, 1994), the reference predicament for identifying both spatial and temporal information from ERP recordings becomes somewhat more obvious when comparing modality-specific ERP components having distinct regional generators (e.g., visual ERP activity is significantly reduced over secondary visual areas with a linked-mastoids reference). Using multiple reference schemes may be helpful for the recognition and appreciation of distinct ERP components, but will not ultimately solve the reference problem; rather, this strategy poses new issues with regard to ERP component quantification and their statistical analyses.

The purpose of the ERP component construct is to decompose ERP waveforms with regard to the underlying neuronal generator(s) and the experimental manipulations, which implies that an ERP component is characterized by temporal (latency), spatial (scalp topography), and functional (condition dependency) specificity (e.g., Donchin et al., 1977; Donchin, Ritter, & McCallum, 1978; Fabiani, Gratton, & Coles, 2000; Picton et al., 2000). However, the identification and measurements of "obvious" waveform peaks as meaningful entities can be misleading. Specifying peaks in noisy waveforms or determining area integration limits for deflections that invert and shift across scalp locations are subject to experimenter bias and raise questions of statistical independency. These problems are magnified with dense EEG montages, adding the problem of how to select or combine channels for ERP component measurement. In dealing with this spatial-redundancy issue, statistical analyses typically adopt a "region-of-interest" approach, in which the ERP signal is reduced to a few spatially smeared sites, thereby again subjecting data analysis to experimenter bias and contradicting the original rationale for an increased spatial signal (Kayser & Tenke, 2005). Despite a general awareness of these issues, the continued use of traditional area, peak, and latency measures becomes increasingly unsatisfactory when one acknowledges that the choice for the reference location is arbitrary.

Reference-Free Components: Current Source Density and Principal Components Analysis

These limitations can be overcome by combining reference-free current source density (CSD) transformations and temporal principal components analysis (PCA) to identify relevant, data-driven components (Kayser & Tenke, 2006c, 2006d; Kayser et al., 2006). The CSD algorithm computes an estimate of the current injected radially into the skull and scalp from the underlying neuronal tissue (i.e., the surface Laplacian) at a given location, from a spatially weighted sum of the potential gradients from all recording sites (negative second spatial derivative; see Tenke & Kayser, 2005, for further details). CSD maps represent the magnitude of the radial current flow entering (sources) and leaving (sinks) the scalp (Nunez, 1981; Nunez & Srinivasan, 2006). The benefits of a CSD transform are a reference-free, spatially enhanced representation of the direction, location, and intensity of current generators that underlie an ERP topography (Mitzdorf, 1985; Nicholson, 1973). By virtue of the algorithm, any surface potential (ERP) reference montage will produce identical CSD waveforms. Compared to more complex EEG source localization methods (Michel et al., 2004), surface Laplacian estimates are more conservative because they completely avoid additional (and unproven) biophysical assumptions (tissue conductivity and geometry, laminar orientation, number and independence of generators). Although a CSD transform can be independently applied to any sample point, cognitive ERP research has mostly used CSD methods to approximate radial currents that underlie a given ERP topography, for instance, as an additional visualization tool to obtain a sharper topographic representation. In contrast, intracranial ERP/CSD research has long also taken advantage of the temporal variation of the neuronal origin of the scalp-recorded field potentials to separate the generator contributions of cortical sublaminae (e.g., Mitzdorf, 1985). However, focusing on CSD waveforms rather than CSD topographies, that is, exploiting the temporal (real-time) sequence of sharpened, reference-free current flow topographies, may also be extremely informative in cognitive ERP research.

Temporal PCA with Varimax rotation is a widely used, systematic, and "data-driven" approach of reducing the dimensionality of ERP waveforms (e.g., Chapman & McCrary, 1995; Donchin, 1966; Donchin & Heffley, 1978; Glaser & Ruchkin,

[1]Whereas an average reference would approximate a "reference-free" recording if sampled with sufficient spatial density (Lehmann, 1984; Pascual-Marqui & Lehmann, 1993), due to the obvious practical limits in sampling from the ventral side of the brain case, a montage-dependent average reference compromise may avoid only some of the pitfalls inherent to a monopolar reference (e.g., Dien, 1998; Junghöfer, Elbert, Tucker, & Braun, 1999).

1976; Kayser & Tenke, 2003; van Boxtel, 1998). This procedure identifies unique and orthogonal variance patterns in the raw data, which are not necessarily evident in grand mean averages due to the overwhelming temporal and spatial complexity of multichannel data sets. Temporal PCA not only aids in determining what are the relevant and statistically independent components within a given data set (factor loadings), it also generates efficient measurements for these overlapping components (factor scores). Factor scores can be reassembled as component topographies for each condition and subject and, together with the time course of the factor loadings, related to the averaged ERP activity. Because of the a priori known temporal organization of the data, the extracted factors can be interpreted as observational definitions of ERP/CSD components if their temporal (loadings) and spatial (scores) characteristics comply with common knowledge of ERP components. Unrestricted PCA solutions, obtained after Varimax rotation of *all* extracted covariance loadings accounting for the total variance, are particularly helpful to establish stable and meaningful observational component definitions (for detailed discussions, see Kayser & Tenke, 2003, 2006a). This greatly reduces the researcher's subjectivity to determining the appropriateness of the observed ERP/CSD measures, rather than having the burden of identifying and justifying the appropriateness and uniqueness (i.e., statistical independence) of an ERP measure within a given data set, all of which are implicit in a traditional ERP measure.

CSD-PCA is a superior, generic approach because different reference schemes will produce different ERP-PCA solutions, but *all* will result in the same unique PCA solution after CSD transformation. Whereas no information is distorted or lost, CSD-PCA can provide new, anatomically appropriate insights into well-studied ERP phenomena (Kayser & Tenke, 2006c; Kayser et al., 2006).

The Present Study

The purpose of the present study was to exploit the advantages of this new CSD-PCA approach for an improved characterization of old/new effects using ERP topographies observed during closely matched auditory and visual continuous word recognition memory tasks. In an initial study using these tasks as a within-subjects paradigm (Kayser et al., 2003), we found highly comparable old/new effects for both modalities despite prominent differences in scalp topography and peak latency of auditory and visual N2 and P3 amplitudes, suggesting that word retrieval as a common, high-level cognitive process is largely independent from but superimposed on the modality-specific ERP component structure. Whereas this report examined the modality-specific properties of the ERP old/new effect, a question not previously addressed, the topographic analysis was limited by using an ERP reference (nose, linked mastoids) and by focusing on midline sites. Furthermore, response latencies were notably longer (about 200 ms) in the auditory than in the visual task, particularly for new items, which was paralleled by a longer peak latency for auditory than for visual P3. Although the peak latencies of the old/new effect were strikingly similar across modalities, the association between response and P3 latency combined with modality-specific response latencies may influence the comparison of old/new effects across modalities. Previous studies have used parallel analysis of stimulus-locked and response-locked ERPs to disentangle the associated functional processes (for review, see, e.g., Johansson & Mecklinger, 2003). A main problem, of course, is that the response-locked activity is superimposed on the stimulus-locked activity, which creates substantial problems for finding a "neutral" baseline for response-locked ERP averages, because a baseline immediately preceding the response (e.g., Nessler & Mecklinger, 2003) or one that includes pre- and postresponse activity will likely reflect an averaged and perhaps condition-specific topography, which is implicitly subtracted from the response-locked ERP signal (for an excellent discussion of this issue, see Urbach & Kutas, 2006). Another problem is the difficulty of directly relating response- and stimulus-locked ERP components when using separate analyses because of their mutual interdependencies. To tackle these problems, the present study employed a joint analysis of stimulus- and response-locked activity by concatenating these waveforms using the same *prestimulus* baseline. The hope was that shared and unique contributions of stimulus- and response-related processes could be identified and disentangled through multiple or unique PCA loading peaks.

Finally, as another advancement in ERP methodology, the rather large sample size ($N = 40$) exceeding the number of recording sites (31) included in the present EEG montage enabled us to evaluate statistical effects by establishing a randomization distribution from the observed data (Maris, 2004). First, randomizations of complete component topographies avoid questionable assumptions about the probability distribution underlying any statistical significance test. Second, and more importantly, because CSD transformations result in more focal activity, potentially revealing statistical effects for different conditions and/or interactions over different regions, randomization tests also avoid an experimenter bias in selecting an appropriate analytical design (e.g., which and how many scalp locations to include in what ANOVA model).

Methods

Participants

Forty-four healthy, right-handed volunteers without a history of neurological illness or substance abuse and without current or past psychopathology based on a standard screening interview (SCID-NP; First, Spitzer, Gibbon, & Williams, 1996) were recruited for the study from the New York metropolitan area. Participants, who were paid US$15/h, had normal or corrected-to-normal vision. Hearing acuity was assessed using standard audiometric procedures, requiring all participants to have an ear difference of less than 10 dB and a hearing loss no greater than 25 dB at 500, 1000, or 2000 Hz. Four subjects had to be excluded because of EEG data loss or excessive EEG artifacts and recording noise, yielding an insufficient number of artifact-free trials (more than 10 in any experimental condition) to compute stable ERP waveforms. The final sample consisted of 40 participants (19 men) ranging in age from 19 to 46 years (mean = 28.6, $SD = 6.8$). Mean education level was 16.0 years ($SD = 2.1$). The mean laterality quotient of the Edinburgh Handedness Inventory (Oldfield, 1971), which can vary between -100.0 (completely left-handed) and $+100.0$ (completely right-handed), was $+80.5$ ($SD = 22.5$). The experimental protocol had been approved by the institutional review board and was undertaken with the understanding and written consent of each participant.

Stimuli and Procedure

This study employed essentially the same auditory and visual continuous word recognition memory paradigm used in our previous study (Kayser et al., 2003). During the serial presentation

of words, participants indicated for each word whether it was new (never presented in the series) or old (presented previously) by pressing one of two buttons on a response pad. Words were presented as auditory or visual stimuli and arranged in four separate blocks (114 trials each, 456 trials total, two auditory and two visual blocks or sequences).

Stimuli consisted of 320 English nouns selected from the MRC Psycholinguistic database (Coltheart, 1981) with a word frequency range of 50–375 per million (Kucera & Francis, 1967) and a concreteness rating range between 247 and 670 (Paivio, Yuille, & Madigan, 1968). These nouns had been randomly assigned to four lists of 80 unique words with the constraint that values for word frequency and concreteness were balanced across lists. For each list, an item sequence was constructed so that an equal number of words ($n = 17$) was repeated once following either a short lag (8 intervening items) or a long lag (24 intervening items). Thus, each sequence had 34 words that repeated once, 17 at each lag, and 46 filler words that did not repeat, yielding a total of 114 items per sequence. Whereas an alternating lag length is a crucial aspect of the stimulus sequencing algorithm, it also assures a greater degree of indeterminancy and was originally intended as a manipulation of task difficulty suitable to study psychiatric populations (Kayser et al., 1999). Items that were to be repeated were considered *new* items at the first presentation, and *old* items at the second presentation, and these repeated items formed the basis for the subsequent data analysis to compare ''true'' memory effects that are largely independent of the physical and connotational differences between stimuli. In contrast, never-repeated words were considered *filler* items and not included in the data analysis. Although fillers are technically also new items, they are, unlike the initial (new) presentation of repeated items, not directly matched to old items. It is therefore preferable to exclude filler items when operationalizing the old/new construct, and at the same time also avoid the comparison of conditions with different signal-to-noise ratios. Word presentation order was pseudorandomized within each sequence to yield an equal distribution of short and long lags.

List and modality assignments were counterbalanced across participants. Therefore, although each stimulus was presented to both auditory and visual modalities across different subjects, for each participant, no single word stimulus was repeated either within or between modalities, except for the new–old item repetitions.

In the auditory condition, sound files of word items (median duration = 484 ms; range = 311–830 ms) were generated for a male voice at a sampling rate of 12 kHz using a publicly available text-to-speech synthesizer (Lucent Technologies, 2001) to control for the variability in emotionality and intonation that occurs in a human voice. The sound files were presented binaurally through headphones at a comfortable listening level of about 72 dB SPL. In the visual condition, graphic files showing word items in black on a light gray background were foveally presented on a CRT computer monitor (500 ms duration), subtending a vertical angle of 0.95°, and horizontal angles ranging from 3.3 to 8.7°.

For both modalities, a constant 2.5-s stimulus onset asynchrony was used. Throughout the auditory task, a fixation cross was visible in the center of the screen to minimize eye movements. Participants were instructed to respond to every stimulus as quickly and accurately as possible and that there would be no overlap between blocks for word repetitions. Responses were accepted from 200 ms poststimulus onset until the next stimulus onset (2500 ms). Response hand assignment (i.e., left/right button press for old/new responses) was systematically alternated across blocks but balanced within participants across modalities, whereas presentation order of auditory (A) or visual (V) modality was counterbalanced across participants (i.e., AVVA or VAAV; for further procedural and permutation details, see Kayser et al., 2003).

Data Acquisition, Recording, and Artifact Procedures

Using a Lycra stretch cap with tin electrodes, nose-referenced scalp EEG (AFz ground) was continuously recorded at 200 samples/s from 30 extended 10–20 system locations (4 midline [Fz, Cz, Pz, Oz] and 13 lateral pairs of electrodes [FP1/2, F3/4, F7/8, FC5/6, FT9/10, C3/4, T7/8, CP5/6, TP9/10, P3/4, P7/8, P9/10, O1/2]; Pivik et al., 1993). Bipolar recordings above and below the right eye and from the outer canthi of each eye monitored vertical and horizontal eye movements. All electrode impedances were kept at or below 5 kΩ. Continuous EEG and EOG data, along with stimulus trigger codes and responses, were recorded through a Grass/Neuroscan acquisition system at a gain of 10k (5k for horizontal and 2k for vertical eye channels) within 0.1–30 Hz (− 6dB/octave). Volume-conducted blink artifacts were effectively removed from the raw EEG using a spatial singular value decomposition filter generated from identified blinks and artifact-free EEG periods, thereby minimizing topographic distortions (NeuroScan, 2003).

Recording epochs of 2000 ms (including a 300-ms prestimulus baseline) were extracted off-line from the blink-corrected continuous data, tagged for A/D saturation, and low-pass filtered at 20 Hz (− 24 dB/octave). To maximize the number of artifact-free epochs, volume-conducted horizontal eye movements, which were systematically prompted in the visual condition (i.e., reading the word stimuli), were reduced by computing the linear regressions between the horizontal EOG and the EEG differences of homologous lateral recording sites (i.e., Fp2 − Fp1, F8 − F7, etc.) for each epoch, and the correlated eye activity was then removed by applying ± beta weight/2 to each lateral EEG signal (cf. Kayser et al., 2006). Furthermore, a reference-free approach was used to identify EEG channels containing amplifier drift, residual eye activity, and muscle- or movement-related artifacts for any given trial (Kayser & Tenke, 2006b), and these artifactual surface potentials were replaced by spherical spline interpolation (Perrin, Pernier, Bertrand, & Echallier, 1989) using the data from artifact-free channels. A trial was rejected if it contained artifact in more than eight channels. Artifact detection and electrode replacement were verified by visual inspection.

Stimulus-locked ERP waveforms were averaged from correct, artifact-free trials using the entire 2-s epoch. The mean number of trials used to compute new and old ERP averages for each lag were 27.9 ($SD = 4.3$, range 14–34) for auditory stimuli and 26.7 ($SD = 5.2$, range 11–34) for visual stimuli. As expected, slightly more trials entered into new (28.6 ± 4.2) than old (26.0 ± 5.0) ERP averages, $F(1,38) = 12.7$, $p = .001$, but the number of old trials were nonetheless sufficient for each condition. Visual inspections of the individual ERP waveforms also confirmed a satisfactory signal-to-noise ratio for each participant. ERP waveforms were screened for electrolyte bridges (Tenke & Kayser, 2001), low-pass filtered at 12.5 Hz (− 24 dB/octave), and finally baseline corrected using the 100 ms preceding stimulus onset.

Response-locked ERP waveforms were averaged from 1-s subepochs including 700 ms before and 300 ms after the recorded response and by applying the stimulus-locked baseline

correction. Trials with responses faster than 400 ms or slower than 1400 ms (9.6% of all trials) had to be excluded when computing response-locked ERPs, because of insufficient sample points at the beginning or end of the subepochs.

Current Source Density

All averaged ERP waveforms at each electrode were transformed into reference-free CSD estimates ($\mu V/cm^2$ units; 10 cm head radius) using a spherical spline surface Laplacian (Perrin et al., 1989) with computation parameters (50 iterations; $m = 4$; smoothing constant $\lambda = 10^{-5}$) previously established for a 31-channel recording montage (e.g., Kayser & Tenke, 2006c; Tenke et al., 1998). By eliminating volume-conducted contributions from distant regions, CSD topographies have more sharply localized peaks than scalp potential (ERP) topographies. Although CSD analysis is montage dependent, due to the relative loss of spatial resolution when averaging across individual topographies, which results in a spatial low-pass filter, surprisingly accurate and reliable surface Laplacian estimates can be obtained for low-density (31-channel) ERP recordings, revealing effectively identical estimates at these sites when compared with CSD obtained from high-density (129-channel) ERPs (Kayser & Tenke, 2006d). Low-density CSDs are adequate and sufficient to summarize group data and therefore capable of providing new insights and superior understandings of ERP data (e.g., Babiloni et al., 2001; Cincotti et al., 2004; Kayser & Tenke, 2006c; Kayser et al., 2006).

Data Reduction and Analysis

To determine common sources of variance in the reference-free transformations of the original ERP data, the averaged CSD waveforms were submitted to temporal PCA derived from the covariance matrix, followed by unrestricted Varimax rotation of the covariance loadings. However, only a limited number of meaningful, high-variance CSD factors are retained for further statistical analysis (for complete rationale, see Kayser & Tenke, 2003, 2005, 2006a, 2006c). Because the extracted CSD factors are independent of the recording reference, they have an unambiguous component polarity and topography.

Although previous research has separately focused on either stimulus- or response-locked ERP activity, a combined analysis would be helpful to better understand the interdependence of stimulus- and response-locked CSD components. For this reason, the stimulus-locked CSD waveforms (400 sample points spanning the time interval from -300 to 1695 ms around stimulus onset) and the response-locked CSD waveforms (201 sample points spanning the time interval from -700 to 300 ms around response onset) were concatenated. It was expected that unique loading patterns would identify ERP activity with an exclusively stimulus-locked (e.g., N1) or response-locked (e.g., response-related negativity) origin or with contributions from both (e.g., P3). This approach allows an evaluation of relative stimulus- and response-locked contributions and provides factor scores as a joint measure for these CSD components to evaluate the topographies of old/new effects. A separate temporal PCA was computed for auditory and visual stimuli to better account for the modality-dependent ERP/CSD component structure (MatLab emulation of BMDP-4M algorithms; cf. appendix of Kayser & Tenke, 2003). Each input data matrix consisted of 601 variables (combined time interval 3005 ms) and 4960 observations stemming from 40 participants, 4 conditions (new/old × short/long lag) and 31 electrode sites, including the nose.

Additional temporal PCAs were separately computed for stimulus- and response-locked CSD waveforms. Because the extracted factors and the ensuing statistical analysis were entirely consistent with the extracted factors and statistical results stemming from the combined CSD waveforms and because the former lack the possibility of directly relating corresponding stimulus- and response-locked factors, only the findings for the combined analysis are reported.

Statistical Analysis

Repeated measures analysis of variance (ANOVA) is typically the method of choice for comparing experimental effects at selected sites deemed suitable for any given ERP component. This requires crucial a priori decisions of which sites to include and which ANOVA design to use (e.g., using lateral and midline sites in the same or different model or mixing regional and hemisphere ANOVA factors), which may or may not be suitable for optimally evaluating any given effect (e.g., the topography of main effects may differ from the topography of interaction effects). The problem of choosing the optimal sites is heightened by the use of CSD measures, which have sharper topographies and lack the spatial redundancies of volume-conducted surface potentials. Moreover, it is always questionable whether all of the assumptions underlying the reference distributions used for parametric F statistics are met by the analyzed data. For these reasons, effects of interest were evaluated by means of randomization distributions estimated from the observed data, which do not depend on any auxiliary assumption (Maris, 2004).

A scaled multivariate T^2 statistic was computed to evaluate topographic old/new differences for paired samples (cf. equation 3 in Maris, 2004):

$$T^2 = \frac{(\overline{y_1} - \overline{y_2})^t \left[\frac{1}{n} S_{diff}\right]^{-1} (\overline{y_1} - \overline{y_2})}{M}, \qquad (1)$$

where $\overline{y_1}$ and $\overline{y_2}$ are the means of the multichannel measurements y_{1i} and y_{2i} ($i = 1, \ldots, n$) of two conditions, each a column vector of M sites (in this case, new and old factor scores pooled across short and long lags at 31 sites for $n = 40$ participants). The symbol S_{diff} denotes the variance–covariance matrix of the differences $y_{1i} - y_{2i}$. Vector transpose and matrix inversion are denoted by ^{t} and $^{-1}$, respectively. In deviation from the conventional computation of a multivariate T^2 statistic, a scaling factor of $1/M$ was applied to allow for direct comparisons of this statistic between (a) EEG montages of different dimensionality, and (b) the univariate (channel-specific) T^2 statistic for paired samples, which is given by:

$$T^2 = \frac{(\overline{y_1} - \overline{y_2})}{\frac{1}{n} s^2}, \qquad (2)$$

where s^2 is the variance of the difference vector.

For each analyzed PCA factor, a paired samples randomization T^2 distribution was approximated by repeatedly (10,000 times) computing the multivariate T^2 statistic (Equation 1) after randomly multiplying the observed old/new difference for each participant by $+1$ or -1. Whereas this multivariate statistic critically evaluates within-subjects condition differences of a complete topography and may be informative if, and only if, the topographic signature is highly similar in the two conditions, the current approach of using data-driven dependent measures in the form of PCA factors renders this overall test of secondary interest. Rather, the more important question of localizing old/new

differences for meaningful CSD variance (i. e., PCA factors) was addressed by estimating the maximum randomization distribution of the univariate (channel-specific) T^2 statistic for paired samples (Equation 2), which consists of only the maxima of the M squared T statistics observed for each repetition. This Scheffé-like post hoc testing procedure controls the family-wise error rate for all channels jointly, thereby avoiding the undesirable decrease in power that would otherwise ensue with Bonferroni correction (Maris, 2004).

Given that randomization testing of ERP topographies represents, as of yet, a rather unconventional, although arguably preferable, statistical approach, factor scores of meaningful PCA factors for each modality were also submitted to repeated measures ANOVA with condition (old, new) and lag (short, long) as within-subjects factors and gender (male, female) as a between-subjects factor. Lag, emerging as an insufficient manipulation of task difficulty (see behavioral data below) and gender were entered as control factors but not considered further. Because these conventional statistics were primarily used for validation, the ANOVA designs included subsets of recording sites at which PCA factor scores had revealed significant old/new effects with the randomization tests. Subsets consisted of either midline sites or lateral, homologous recording sites over both hemispheres, thus adding either site or site and hemisphere as within-subjects factors to the design. Greenhouse–Geisser epsilon (ε) correction was used to compensate for violations of sphericity when appropriate (e.g., Keselman, 1998). If necessary, sources of interactions and main effects were explored with simple effects (BMDP-4V; Dixon, 1992). A conventional significance level ($p < .05$) was applied for all effects.

For analyses of the behavioral data, response latency (mean response time of correct responses) and percentages of correct responses were submitted to repeated measures ANOVA with condition (old, new), lag (short, long), and modality (visual, auditory) as within-subjects factors and gender as the between-subjects factor. As in our previous word recognition memory studies (Kayser et al., 1999, 2003), the d'-like sensitivity measure d_L was calculated from hit and false alarm rates (Snodgrass & Corwin, 1988) and submitted to a similar ANOVA without the condition factor.

Results

Behavioral Data

Table 1 summarizes the behavioral performance for both modalities, which closely matched our previous findings (Kayser et al., 2003). Participants distinguished old from new items well above chance, as can be seen from both the correct responses for old items and the sensitivity measure (d_L), and these accuracy measures revealed no differences between the visual and auditory modality. As expected, however, mean response latency was significantly shorter in the visual than auditory task, particularly for new items (more than 300 ms).

For old items only, a slightly better hit rate was observed for short compared to long lags (84.5% vs. 81.4%), Condition × Lag interaction, $F(1,38) = 5.63$, $p = .02$. However, there was no effect involving lag for d_L, suggesting that the former effect was due to differences in response bias. Although lag also impacted on response latency, lag main effect, $F(1,38) = 5.93$, $p = .02$; Condition × Lag interaction, $F(1,38) = 8.69$, $p = .005$, the observed differences were, by comparison, rather small and not very meaningful ($M \pm SD$, short vs. long lag, new 805 ± 220 vs. 785 ± 221 ms; old 801 ± 191 vs. 802 ± 189 ms). Given the lack of accuracy/sensitivity and meaningful response latency differences as a function of lag, electrophysiologic measures were pooled across lag to reduce the complexity of the design (cf. Kayser et al., 2003).

Table 1. *Behavioral Data Summary: Grand Means (SD) and ANOVA F Ratios*

	Correct responses (%)		Sensitivity	Latency (ms)	
Modality	New	Old	[d_L]	New	Old
Auditory	92.3 (7.6)	84.0 (13.7)	4.56 (1.12)	952 (160)	914 (160)
Visual	91.4 (10.5)	81.8 (14.0)	4.41 (1.50)	638 (148)	689 (145)

Effect[a]	F	p	F	p	F	p
Modality					386.72	$< .0001$
Condition[b]	15.1	.0004	—	—		
Modality × Condition[b]			—	—	50.91	$< .0001$

[a]For all effects, $df = 1,38$. Only F ratios with $p < .10$ are reported.
[b]Not applicable to d_L sensitivity measure.

Average ERP and CSD Waveforms

Figure 1 shows the grand average, nose-referenced ERP waveforms of stimulus-locked and response-locked surface potentials for auditory and visual stimuli, collapsed across condition and lag. The overall stimulus-locked ERP deflections were highly comparable to our prior study (see Figures 2 and 3 in Kayser et al., 2003). For the auditory task (dashed lines), distinctive stimulus-locked ERP components were identified as N1, P2, and N2, particularly over central sites (e.g., see Cz in Figure 1A), and as P3 and a late negativity (LN) over posterior sites (e.g., see site P3 in Figure 1A). For the visual task (gray lines), distinctive stimulus-locked ERP components were identified as P1, N1, and N2, particularly over inferior-parietal sites (e.g., see P9 in Figure 1A), and as P3 and LN over posterior sites (e.g., see Pz in Figure 1A). As can be seen, peak latencies and topographies of individual stimulus-locked components varied according to modality. In contrast, the response-locked ERP component structure was less modality dependent, including a distinct mid-parietal positivity with a maximum at response onset (see Pz in Figure 1B) and a prominent mid-frontal negativity (FRN, frontal response negativity) that peaked at approximately 50 ms after response onset and terminated the preceding parietal positivity (see Fz in Figure 1B).

Although horizontal and vertical eye movements differed across modalities, it is clear that blink activity was effectively removed by the spatial blink filter applied to the continuous data and did not differentially affect ERPs. Given the use of a nose reference, ERP components were smaller at frontal compared to posterior sites, whereas a linked-mastoids reference (i.e., the mean of sites TP9 and TP10) would yield an inverted potential at frontal sites, mostly affecting visual ERPs (i.e., a different reference will result in a different pattern of positive and negative ERP activity and will differentially impact on visual and auditory ERPs).[2]

[2]Animated topographies of stimulus- and response-locked CSD waveforms can be obtained at http://psychophysiology.cpmc.columbia.edu/cwrm2006csd.html. For comparability to previous research, animated stimulus- and response-locked topographies of ERP surface potentials using a linked-mastoids reference are also available.

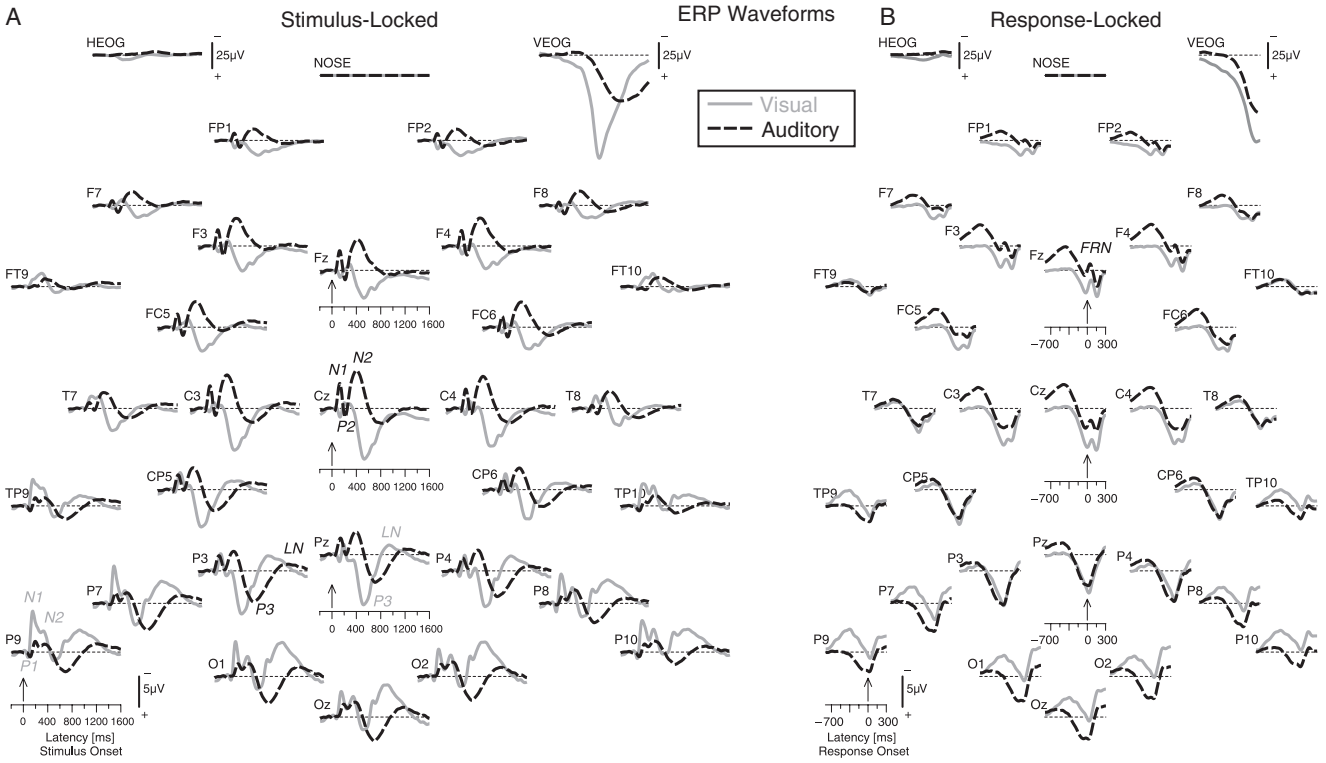

Figure 1. Stimulus-locked (− 200 to 1600 ms) (A) and response-locked (− 700 to 300 ms) (B) grand average event-related surface potential (ERP) (in microvolts) waveforms ($N = 40$) for visual and auditory stimuli (averaged across old and new items) at all 30 recording sites using a nose tip reference (100 ms prestimulus baseline for both). Horizontal and vertical electrooculograms (EOG) are shown at a smaller scale before blink correction. Stimulus-specific ERP components were well defined over the posterior scalp for the visual modality (P1, N1, N2, and P3 are labeled at sites P9 and Pz), and over centro-posterior regions for the auditory modality (N1, P2, N2, and P3; see Cz and P3). For both modalities, P3 was followed by a late negativity (LN), and a distinct response-specific negativity was evident over mid-frontal sites (FRN; see Fz).

The reference-free CSD transformations of these ERP waveforms, which eliminate these reference-dependent ambiguities, are presented in Figures 2 and 3, showing sink (negative) and source (positive) activity for new and old stimuli at each recording site. Distinct stimulus-locked auditory CSD components (Figure 2A) included central N1 and N2 sinks (approximate peak latencies 120 and 420 ms at C3), a central P2 source (205 ms at Cz), a lateral-posterior P3 source (635 ms at P7), and a late mid-parietal sink (1100 ms at Pz) for old stimuli only. Increased lateral-parietal P3 sources (at P3, P7) for old compared to new stimuli were accompanied by increased lateral-frontal sinks (at F7, F8). This prominent source-sink pattern of old/new effects was also evident for the response-locked auditory CSDs (Figure 2B), peaking at approximately 145 ms prior to response onset.

Prominent stimulus-locked visual CSD components (Figure 3A) included inferior lateral-parietal P1 sources (approximate peak latency 80 ms at P8) and N1 sinks (150 ms at P7), followed by an occipital P2 source (195 ms at Oz) and central N2 sink (270 ms at Cz). Increased mid-parietal P3 sources (500 ms at Pz) for old compared to new stimuli were accompanied by increased lateral-frontal sinks (at F7, F8), and this old/new source-sink pattern was again present in the response-locked visual CSDs (Figure 3B), peaking at approximately 140 ms prior to response onset.

CSD difference waveforms (i.e., old minus new), which represent the time courses of the reference-free old/new effects for visual and auditory tasks (Figure 4), were remarkably similar across modalities. Stimulus-locked old/new effects were largely characterized at mid-parietal sites by a difference waveform of positive and negative amplitudes peaking at approximately 600 and 1200 ms, respectively (see site P3 in Figure 4A). By and large, this pattern coincided with inverted differences at lateral-frontal sites (F7/8, FT9/10). These observations seemed to hold for response-locked old/new effects, particularly for the auditory task (Figure 4B). A sharp inversion of positive-going old/new differences occurred at mid-frontocentral sites (Fz, Cz) immediately after response onset, indicating that the FRN sink activity was greater at Fz for old than new items, independent of stimulus modality.

PCA Component Waveforms and Topographies

In Figures 5 and 6, the time courses of factor loadings (panels C, D) and corresponding factor score topographies (E) for the first nine CSD factors extracted for each modality (more than 85% explained variance after rotation for each PCA solution) are compared to stimulus- and response-locked CSD waveforms at characteristic sites (A, B). Although combined CSDs were submitted to the PCA, the resulting factor loadings were separately displayed for their stimulus- and response-locked portions using appropriate time scales to facilitate interpretation (Figures 5C, D and 6C, D). At first glance, the information extracted in these analyses may seem overwhelming; however, both PCA solutions revealed rather simple and almost parallel sets of factors with unique stimulus- *or* response-locked loading peaks (solid lines in

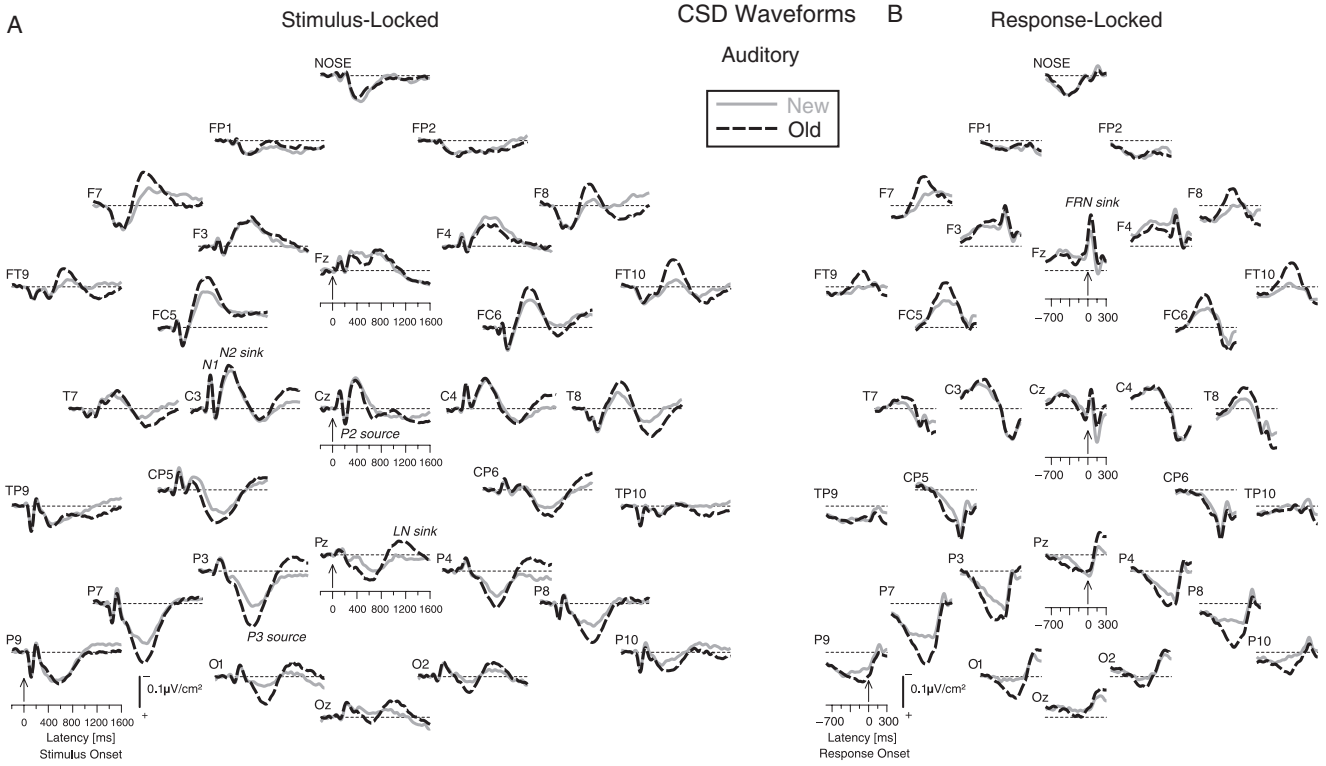

Figure 2. Stimulus- (A) and response-locked (B) reference-free current source density (CSD) (in units of $\mu V/cm^2$) waveforms comparing new and old auditory stimuli at all 31 sites. Distinct CSD components included stimulus-locked central N1 and N2 sinks (approximate peak latencies 120 and 420 ms at C3), central P2 (205 ms at Cz), and lateral-posterior P3 sources (635 ms at P7) and response-locked mid-frontal sinks (45 ms at Fz). Increased lateral-parietal P3 sources (P3, P7) and lateral-frontal sinks (F7, F8) were seen for old compared to new auditory stimuli.

Figures 5C,D and 6C,D) or with both stimulus- *and* response-locked loading peaks (dashed lines in Figures 5C, D and 6C, D). Labels were therefore chosen to indicate the peak latency of the factor loadings relative to stimulus and response onsets. For easy reference and identification, brief functional interpretations of factors were also provided when a signature topography was observed. Chosen labels like ''N1 sink'' and ''P3 source'' were not intended to exclusively refer to these identifying sink and source activities but rather to the respective CSD factors, consisting of characteristic time courses and topographies.

For both modalities, three factors summarized early phasic, stimulus-driven CSD activity. For auditory stimuli, CSD factors corresponded to N1 sink (peak latency 120 ms; left mid-central maximum; 1.1% explained variance), P2 source (210 ms; frontocentral maximum; 2.3%), and N2 sink (360 ms; vertex maximum; 2.7%; Figure 5C,E). Likewise, for visual stimuli, CSD factors corresponded to N1 sink (135 ms; left lateral inferior-parietal maximum; 1.8%), P2 source (195 ms; occipital maximum with lateral-parietal sinks; 2.7%), and N2 sink (265 ms; mid-frontocentral maximum with mid-parietal sources; 2.0%; Figure 6C, E).[3] Notably, all of these factors had no substantial loadings during the response-locked time interval (Figures 5D and 6D).

For both modalities, two high-variance factors summarized primarily cognitive CSD activity that preceded and followed the response. For these components, stimulus- and response-locked contributions were evident from substantial factor loadings during both time intervals. P3 source activity was summarized by factors that peaked 635 ms (auditory) and 465 ms (visual) after stimulus onset (Figures 5C and 6C), which coincided with loadings peaks 170 ms and 140 ms before response onset (Figures 5D and 6D). The P3 source factor for auditory stimuli (29.5% explained variance) corresponded to lateral parietal sources, mostly over the left hemisphere, which were paired with lateral-frontal sinks (Figure 5E); for visual stimuli, the P3 source factor (20.6%) corresponded to medial-parietal and medial-frontopolar sources (Figure 6E). Similarly, LN sink activity was summarized by factors that peaked 815 ms (auditory) and 950 ms (visual) after stimulus onset, which coincided with loadings peaks at 185 ms and 175 ms after response onset (Figures 5D and 6D). These LN sink factors (15.3% and 29.2%) had very similar topographies across modalities, consisting of a prominent occipital sink paired with central-temporal sources.

A high-variance, stimulus-locked slow wave (SW) factor was found for both auditory (1435 ms; 22.2%) and visual stimuli (1510 ms; 21.2%). The response-locked portion of the loadings suggested that these peaks were well beyond response onset, although an increase in loadings' amplitude seemed to start after the response (Figures 5D and 6D). Both SW factors consisted of midline sources paralleled by medial sinks (Figures 5E and 6E).

[3]For the visual task, another low-variance CSD factor clearly corresponded to P1 source (85 ms; lateral-parietal maxima with a mid-occipitoparietal sink; 0.7%). For sake of brevity, and given the lack of old/new effects, this factor was not further considered for this report.

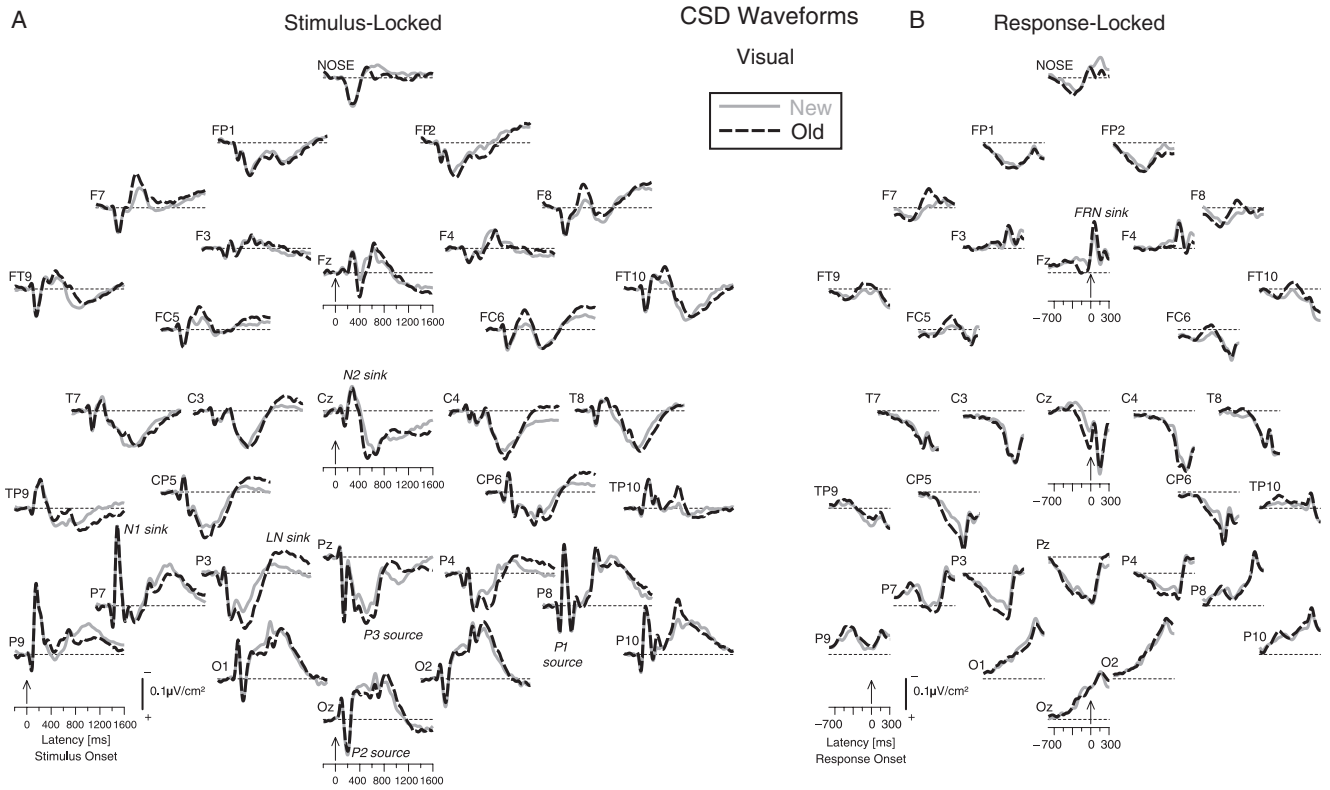

Figure 3. Stimulus- (A) and response-locked (B) CSD waveforms as in Figure 2 for visual stimuli. Distinct CSD components included stimulus-locked inferior lateral-parietal N1 sinks (approximate peak latency 150 ms at P7) and mid-parietal P3 sources (500 ms at Pz) and response-locked mid-frontal sinks (50 ms at Fz). Increased mid-parietal P3 sources (P3, Pz) and lateral-frontal sinks (F7, F8) were seen for old compared to new visual stimuli.

Each PCA solution produced a purely response-locked CSD factor peaking at approximately 40 ms after response onset, with no secondary loadings peak in the stimulus-locked time interval (Figures 5C, D and 6C, D). These two FRN sink factors (1.3% each) corresponded to prominent Fz sink maxima accompanied by centroparietal sources (Figures 5E and 6E).

Finally, both PCA solutions produced another CSD factor with notable loadings peaking at 525 ms (auditory) and 540 ms (visual) before the response onset, but also showing smaller loadings peaks at 395 ms (auditory) and 145 ms (visual) after stimulus onset. These peak patterns were paired with factor score topographies reminiscent of early sink activities, revealing a mid-central N1/N2-like sink pattern for the auditory task and a left-lateralized N1-like sink pattern for the visual task. Although these factors clearly gathered variance (8.3% and 4.6%) associated both with early stimulus-driven and response-locked CSD activity, given their smaller amplitudes and the broader time periods of their loadings, these factors were not further considered in this report. There were also low-variance factors of uncertain origin for auditory (855 ms; 2.4%) and visual (1040 ms; 2.1%) stimuli, but because these factors were not linked to any clear topography, no further analyses were applied.

Randomization Tests of Topographic Old/New Effects

There were no significant old/new effects for N1 sink factors (multivariate auditory $T^2 = 3.77$, visual $T^2 = 5.05$, both $p > .42$; all univariate $T^2 < 5.30$, all $p > .50$). However, significant old/new effects were found for other meaningful CSD factors beginning with the auditory P2 source. Figure 7A shows the findings for auditory CSD factors preceding response onset. Most importantly, for the auditory P3 source factor, the pattern of medial-parietal sources and lateral-frontocentral sinks was clearly more robust for old than new stimuli, resulting in prominent old–new differences at the very same sites, a significant multivariate effect (Figure 7A, row 3). The univariate max(T^2) statistics at each site further corroborated this finding, revealing increased P3 sources at medial-parietal sites (at P7, P8, P3, P4, CP5, P10, all $T^2 > 31.1$, all $p < .0001$) and increased sinks at lateral-frontocentral sites (at F7, F8, FT9, FT10, FC5, all $T^2 > 30.2$, all $p < .0001$).

There were also old/new effects for the auditory P2 source and N2 sink factors, but these effects were clearly weaker and did not parallel the sink-source patterns characteristic for these factors (Figure 7A, rows 1 and 2). For the auditory P2 source, reduced sink activity was found for old compared to new items over lateral-parietal sites (at P7, P3, P10, all $T^2 > 11.5$, all $p < .04$). For the auditory N2 sink, reduced source activity was found for old compared to new items over inferior-parietal sites, primarily for the left hemisphere (at P7, $T^2 = 15.5$, $p = .009$; at P9, $T^2 = 12.2$, $p = .02$; at P8, P10, both $T^2 > 10.0$, both $p < .08$), although the multivariate T^2 statistic failed to indicate a significant overall topographic old/new effect.

Figure 7B shows the old/new effects for visual CSD factors preceding response onset. As for the auditory task, visual P3 sources at mid-parietal and mid-frontocentral sites were larger for old than new stimuli, and so were the accompanying lateral-frontocentral sinks, yielding a significant multivariate effect

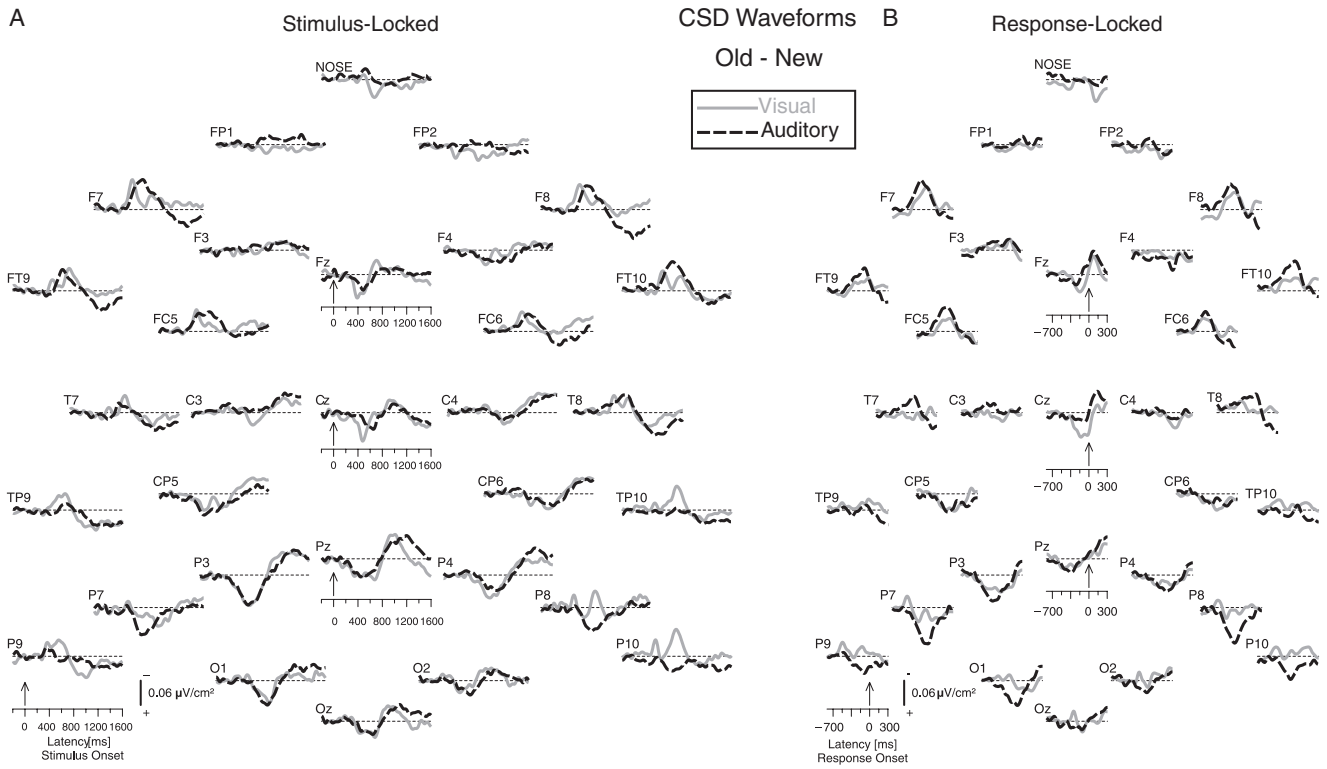

Figure 4. Stimulus- (A) and response-locked (B) old-minus-new CSD difference waveforms showing old/new effects for visual and auditory modalities. Prominent old/new effects common to both modalities were evident at left medial-parietal sites (e.g., P3), but also at lateral-frontal sites (F7, F8), and were also evident for response-locked CSDs.

(Figure 7B, row 3). Accordingly, highly significant univariate max(T^2) statistics corroborated increased P3 sources at midline (at Cz, $T^2 = 45.8$, $p < .0001$; at Fz, $T^2 = 20.3$, $p = .002$; at Pz, $T^2 = 13.0$, $p = .02$) and medial-parietal sites (at P3, P4, both $T^2 > 24.4$, both $p < .0001$; at CP5, $T^2 = 18.1$, $p = .003$) and increased sinks at lateral-frontocentral sites (at F7, F8, FC5, all $T^2 > 26.2$, all $p < .0001$; at FC6, $T^2 = 22.1$, $p = .0005$).

Whereas there were no significant old/new effects for the visual P2 source factor, significant old/new effects were found for the visual N2 sink factor at characteristic sites (Figure 7B, row 2). Greater N2 sink amplitude for old than new items was found at mid-frontocentral sites (at Cz, $T^2 = 16.9$, $p = .006$; at Fz, $T^2 = 14.5$, $p = .01$). There were also two isolated old/new effects for this factor, stemming from reduced sink activity for old than new items at site P9 ($T^2 = 12.8$, $p = .02$) and increased source activity at FC6 ($T^2 = 11.6$, $p = .04$).

For the evaluation of old/new effects that emerged after the response, it was reasoned that the underlying cognitive operations were less affected by the processing modality and therefore likely to be common to both modalities, a consideration that was also supported by the topographic similarities of auditory and visual factors corresponding to FRN sink, LN sink, and SW activity. To increase statistical power, the corresponding factor scores were therefore pooled across modality, and the resulting topographies and statistical old/new effects are shown in Figure 7C.[4] Old items resulted in an increased FRN sink at site Fz compared to new items ($T^2 = 20.5$, $p = .001$), and, at the same time, in a greater source activity at lateral-frontocentral sites (at F7, $T^2 = 23.2$, $p = .0004$; at F8, $T^2 = 18.4$, $p = .003$; at FC6, FT10, both $T^2 > 13.4$, both $p < .02$). In addition, a reduced source activity for old than new items was observed at site P3 ($T^2 = 12.9$, $p = .02$). Although the multivariate T^2 statistic did not indicate a significant overall old/new effect for the FRN sink factor, one must consider that a focal midline factor necessarily reflects considerable local field closure, and this overall topographic analysis is therefore less meaningful.

Finally, significant multivariate T^2 statistics were observed for the LN sink and SW factors (Figure 7C, rows 2 and 3). The topography of the LN sink old/new effects was notably different from the factor's characteristic topography, with reduced midline source activity for old compared with new items (at Cz, Pz, both $T^2 > 22.1$, both $p < .0004$; at Fz, $T^2 = 12.0$, $p = .03$) but increased sources at adjacent sites (at FC6, CP6, both $T^2 > 18.0$, both $p < .003$; at FC5, $T^2 = 11.0$, $p = .049$). SW old/new effects were larger sinks for old compared with new items at central-parietal sites (at P3, $T^2 = 50.0$, $p < .0001$; at C4, P4, both $T^2 > 21.3$, both $p < .0008$; at CP6, $T^2 = 19.5$, $p = .002$; at CP5, $T^2 = 11.5$, $p = .04$), and an increased source at site TP9 ($T^2 = 14.0$, $p = .01$).

Confirmatory Repeated Measures ANOVA

Results of the conventional F tests performed at selected sites, which corresponded to significant topographic old/new effects observed with the randomization tests, are summarized for the different CSD-PCA factors in Table 2. Extremely robust old/new effects were observed for almost all old/new effects reported above (i.e., condition main effect, most $F[1,38] > 24.3$, $p < .0001$),

[4]Separate randomization tests were also performed for these post-response factors for each modality. As these findings were fully consistent with the pooled analyses, only the latter are reported.

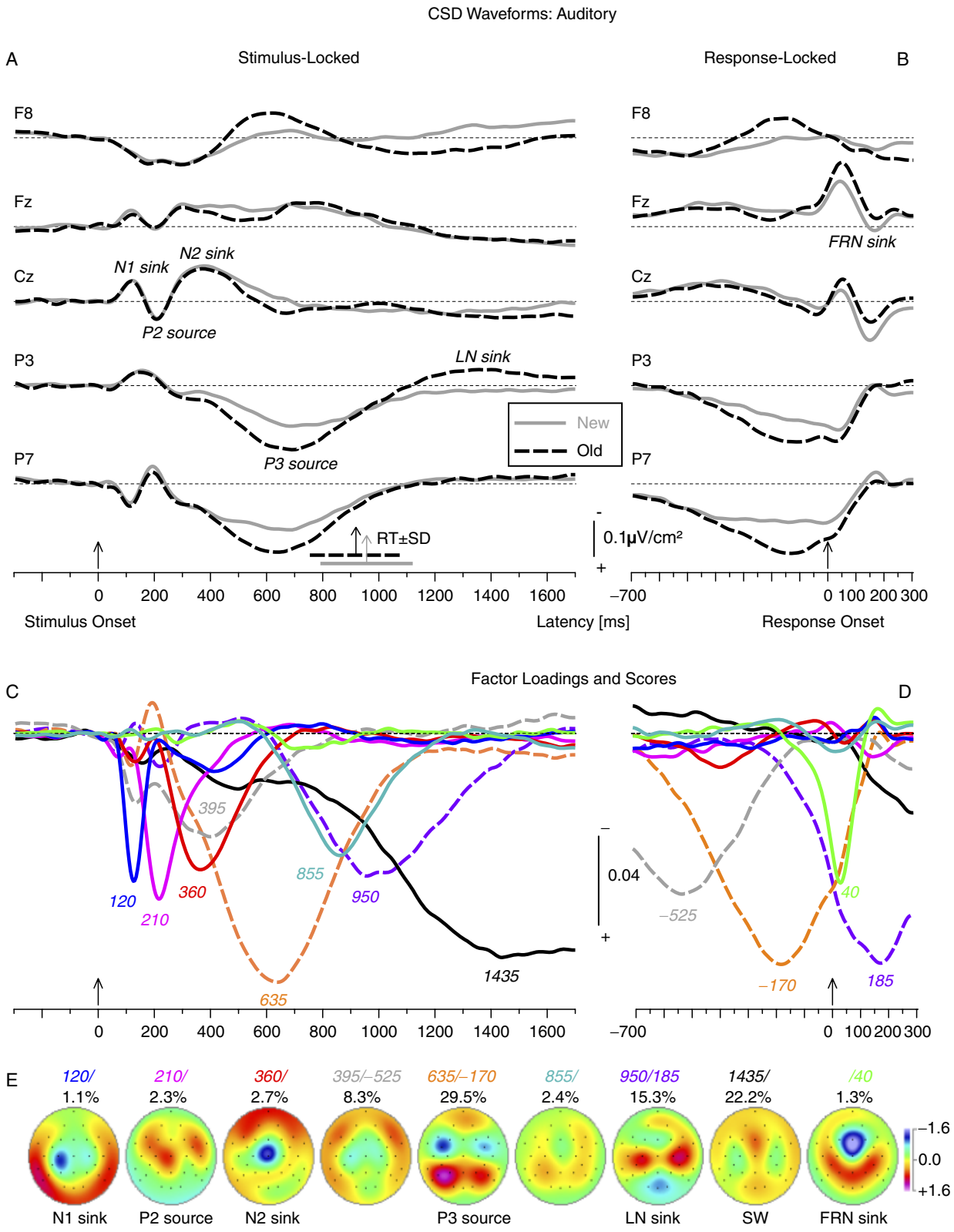

Figure 5. Unrestricted PCA solution using auditory CSD waveforms. Stimulus- (− 300 to 1700 ms) (A) and response-locked (− 700 to 300 ms) (B) grand mean CSDs at selected sites (F8, Fz, Cz, P3, P7) comparing new and old items. Mean response latencies (RT ± *SD*) are marked for stimulus-locked CSDs. C, D: Time courses of Varimax-rotated covariance loadings for the first nine auditory CSD factors extracted (85.2% total variance explained). Labels indicate the peak latency of the factor loadings relative to stimulus and response onsets. Factors with unique stimulus- *or* response-locked loading peaks are indicated by solid lines, whereas factors with both stimulus- *and* response-locked loading peaks are indicated by dashed lines. E: Corresponding factor score topographies (nose at top) with percentage of explained variance. CSD factor labels consist of stimulus- and/or response-locked peak latencies of the factor loadings (brief functional interpretations of factors are based on a signature topography). Topographies are roughly ordered by their temporal sequence, placing the unique response-locked factor at the end. The same symmetric scale was used for all topographic maps.

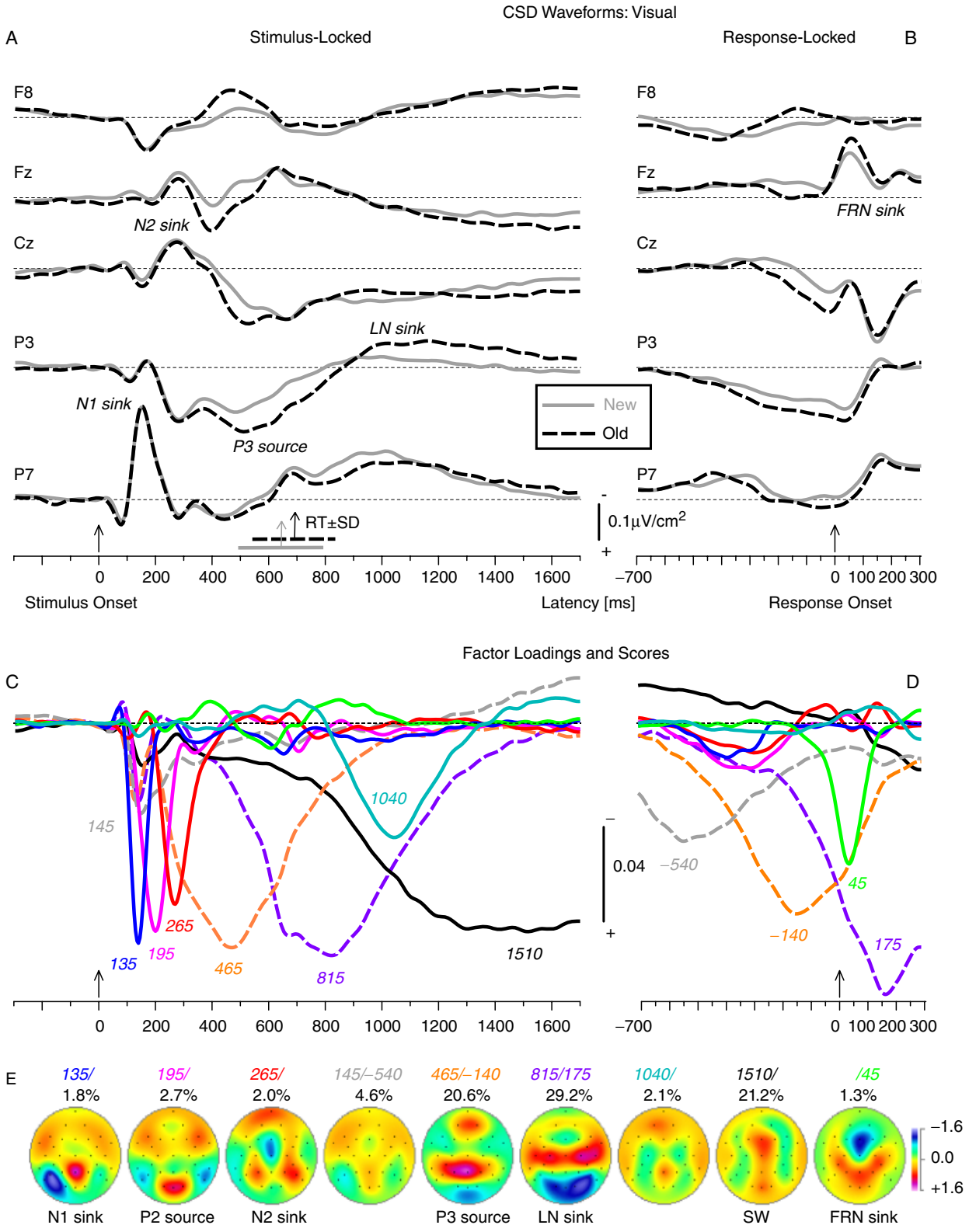

Figure 6. Unrestricted PCA solution as in Figure 5 using visual CSD waveforms. Stimulus- (A) and response-locked (B) grand mean CSDs. C,D: Time courses of Varimax-rotated covariance loadings for the first nine visual CSD factors extracted (85.6% total variance explained). E: Corresponding factor score topographies.

and all reached at least a conventional 5% significance level. Thus, the significance tests derived from randomizations of the observed data, which require no assumptions regarding the underlying data distributions, were found to be consistent with the parametric repeated measures ANOVA, but were apparently more conservative.

Because Condition × Hemisphere and Condition × Hemisphere × Site interactions were not directly probed by the previous randomization tests, the absence of these effects in most of the repeated measures ANOVA is of interest. However, there were also notable exceptions. The analyses for the auditory P3 source factor revealed two highly significant three-way interactions of Condition × Hemisphere × Site (Table 2A). For the lateral-parietal source activity, simple Condition × Hemisphere interaction effects performed at each site were significant at sites P3/4, $F(1,38) = 18.9$, $p = .0001$, CP5/6, $F(1,38) = 12.1$, $p = .001$, and P9/10, $F(1,38) = 5.37$, $p < .03$, but not at P7/8, $F(1,38) < 1.0$. This reflected the greater old/new effects favoring the left hemisphere at P3/4 and CP5/6, but favoring the right hemisphere at P9/10 (Figure 7A, row 3). For the associated lateral-frontal sink activity of this factor, similar simple interaction effects were significant at sites FT9/10, $F(1,38) = 7.89$, $p = .008$, T7/8, $F(1,38) = 5.69$, $p = .02$, and FC5/6, $F(1,38) = 4.15$, $p < .05$, but not at F7/8, $F(1,38) < 1.0$, all resulting from larger sinks for old than new items over the right than left hemisphere.

The analyses for the visual P3 source factor revealed a significant Condition × Hemisphere interaction for the lateral-parietal source activity (Table 2B), stemming from greater sources for old than new items over left medial-centroparietal sites (i.e., CP5/6 and P3/4; Figure 7B, row 3), thereby matching the findings for the auditory P3 source at these sites.

Discussion

By combining several methodological advancements, the current study improved the characterization of ERP old/new effects during matched visual and auditory word recognition tasks, revealing considerable independence from the underlying modality-specific ERP component structure. First, CSD transformations of ERP waveforms provided reference-independent estimates of sink and source activity underlying surface potentials. In close agreement with our previous study (Kayser et al., 2003), distinct ERP components were observed in a parallel temporal sequence for each modality, with modality-specific latencies and distinct topographies corresponding to the anatomy of visual and auditory pathways. This ERP component sequence unambiguously corresponded to distinct CSD components with narrower peak latencies and sharper sink/source topographies. These CSD components provide a conservative, but systematic bridge between surface potentials and their underlying neuroanatomical generators. Second, temporal PCA provided a concise summary of auditory and visual CSD activity (Kayser & Tenke, 2003, 2006c) associated with generator patterns underlying stimulus processing and overlapping episodic memory (old/new effects). Third, and perhaps most importantly, given the longer response latencies to auditory than visual stimuli, which differentially affected old and new items, the combined extraction of stimulus- and response-locked ERP/CSD components allowed a joint, direct evaluation of stimulus- and response-related old/new effects. Response-locked ERPs were not realigned to a poststimulus baseline, which could introduce a confound by subtracting stimulus-locked topographies (original components and/or condition effects; cf. Urbach & Kutas, 2006). Both events (stimulus and response onset) triggered unique and common old/new effects dissociable by their temporal and topographic characteristics. Fourth, an unbiased statistical evaluation of topographical old/new effects was achieved through randomizations of complete component topographies (Maris, 2004), rather than analyzing "representative" regional subsets of recording locations (cf. Kayser & Tenke, 2005). Although we employed a continuous recognition memory paradigm, these improvements are task unspecific and may also benefit study–test and other paradigms.

A prominent left parietal old/new effect was observed in both modalities, overlapping highly distinct auditory and visual P3 sources. Stimulus-locked P3 source peaked approximately 170 ms earlier for visual than auditory tasks, probably due to the longer processing time required for auditory temporal analysis, but both sources preceded the response by about the same amount. P3 sources had distinct parietal topographies, consisting of either midline (visual) or lateral (auditory) maxima, but both included prominent lateral frontocentral sinks. Notably, the generator patterns of the overlapping old/new effects differed from visual P3, including mid-frontocentral and medial-parietal sources, but resembled auditory P3, with off-midline parietal sources. Both old/new topographies also included lateral frontocentral sinks.[5] Whereas these old/new topographies resembled dipole-like generators, with slightly different regional orientations for auditory and visual stimuli, they are likely to indicate activity within a recognition memory network involving frontal and parietal regions (Iidaka, Matsumoto, Nogawa, Yamamoto, & Sadato, 2006). These findings nicely converge with fMRI evidence, consistently implicating old/new effects for the lateral posterior parietal cortex and its medial surface, including precuneus, posterior cingulate, and retrosplenial cortex (Wagner, Shannon, Kahn, & Buckner, 2005).

The parietal old/new *source* effect was more robust over the left than right hemisphere at medial centroparietal sites for both modalities, consistent with previous ERP findings (e.g., Herron, Quayle, & Rugg, 2003; Wilding & Rugg, 1997; Woodruff, Hayama, & Rugg, 2006). In contrast, right-larger-than-left frontal old/new *sink* asymmetries accompanying the parietal old/new source effects were observed for auditory, but not visual, stimuli. Notwithstanding some superficial similarities, the present frontal old/new sink effect should not be confused with the previously reported right frontal old/new effect, which had a later onset, prolonged duration (>1 s), and a positive ERP polarity (e.g., Mecklinger, 2000; Senkfor & Van Petten, 1998; Wilding & Rugg, 1996). For better comparability to previous research, ERP waveforms referenced to nose or linked mastoids, comparing new and old stimuli for each modality at selected sites, are shown in Figure 8. As can be seen, no inverted lateral-frontal old/new effect could be discerned for visual ERPs referenced to nose or linked mastoids (cf. sites F7/8 in Figure 8A, C), suggesting that it is obscured, at least in part, by volume conduction (cf. discussion in Kayser et al., 2003). Rereferencing shifted positive and negative ERP deflections and their peak latencies across scalp

[5] In a strict sense, the distinction between sinks or sources to describe a CSD difference topography is arbitrary because inverting the sign provides an equally meaningful effect description. Nevertheless, the differential generator activity can be correctly expressed with these terms. The same considerations apply to the ERP old/new effect, which is conventionally defined by the difference old minus new.

Table 2. *Summary of F Ratios (and ε Corrections) from Repeated Measures ANOVA Performed on CSD-PCA Factors at Selected Sites*

	A: Auditory Factor Preceding Response Onset (Sites)				
	210/	***360/***	***635/ – 170***		
	P2 source	N2 sink	P3 source		
Variable	(P3/4, P7/8)	(P7/8, P9/10)	(CP5/6, P3/4, P7/8, P9/10)	(F7/8, FT9/10, FC5/6, T7/8)	(Fz, Cz, Pz, Oz)
C	26.70****	24.35****	111.77****	80.09****	25.11****
C × H	2.92		3.77		—
C × S			14.04**** (0.82)	4.12* (0.73)	
C × H × S	3.79		12.04**** (0.84)	5.82** (0.73)	—
H		5.16*	36.75****		—
S			25.08**** (0.55)	18.15**** (0.60)	8.79*** (0.80)
H × S		4.53*	2.71 (0.77)	23.09**** (0.82)	—

	B: Visual Factor Preceding Response Onset (Sites)				
	265/		**465/ – 140**		
	N2 sink		P3 source		
Variable	(Fz, Cz)	(TP9/10)	(CP5/6, P3/4)	(F7/8, FT9/10, FC5/6)	(Fz, Cz, Pz)
C	25.38****	5.74*	41.88****	40.85****	69.08****
C × H	—		4.71*		—
C × S		—	4.68*	8.87*** (0.88)	
C × H × S	—	—			—
H	—	18.37***	20.09***		—
S		—	27.50****		31.77**** (0.94)
H × S	—	—		7.00** (0.87)	—

	C: Pooled Factor Common to Both Modalities Following Response Onset (Sites)					
	FRN sink		LN sink		SW	
Variable	(Fz)	(F7/8, FT9/10, FC5/6)	(Fz, Cz, Pz)	(FC5/6, CP5/6)	(C3/4, CP5/6, P3/4)	(TP9/10)
C	20.48***	41.63****	63.44****	29.81****	71.99****	10.50**
C × H	—		—			3.27
C × S	—	5.48** (0.93)				—
C × H × S	—		—			—
H	—	5.78*	—	23.33****	9.23**	
S	—		23.19**** (0.99)	6.41*	3.26 (0.82)	—
H × S	—	9.69*** (0.98)	—	17.01***	5.88** (0.85)	—

Note. C: condition (new, old); H: hemisphere (left, right); S: electrode site (subsets as indicated). Only *F* ratios with $p < .10$ are reported. For ε-corrected effects, $df = 3,114$ (A) or $df = 2, 76$ (B, C); for all other effects, $df = 1,38$.
—: Effect not applicable.
*$p < .05$; **$p < .01$; ***$p < .001$; ****$p < .0001$.

locations, particularly for visual stimuli, but also for response-locked ERPs (Figure 8B, D). Because early visual components (N1, N2) are maximal over lateral inferior (i.e., secondary visual) cortex when using a nose reference (e.g., Kayser et al., 1999, 2003; cf. site P9 in Figure 8A), choosing an EEG reference at or near this region (i.e., using linked mastoids or ears) inverts and shifts the nose-referenced ERP energy to more remote scalp locations (see peak labeled N1′ at site Cz in Figure 8C; cf. Dien, 1998; Friedman et al., 2005). Although an inverted lateral-frontal old/new effect was recognizable for auditory ERPs with linked-mastoids reference (cf. sites F7/8 in Figure 8C), most of the relevant literature relied on visual ERPs. Thus, the association of a frontal old/new sink with a parietal old/new source constitutes a new finding. In these continuous recognition memory tasks, increased frontal sinks and parietal sources to old items were extracted as a single temporal CSD component, but a temporal

Figure 7. Statistical evaluation of topographic old/new effects using randomization tests for paired samples for (A) three auditory and (B) three visual CSD factors preceding response onset (modality-specific P2 source, N2 sink, P3 source), and (C) for three CSD factors following response onset common to both modalities (FRN sink, LN sink, SWactivity), for which corresponding factor scores were pooled across modality. Shown are the mean factor score topographies for new and old auditory stimuli and their respective old-minus-new difference (multivariate Hotelling's T^2 statistics are reported to the left), and squared univariate (channel-specific) paired samples *T* statistics thresholded at the 95th quantile ($p = .05$) of the corresponding randomization distribution (maximum of all 31-channel squared univariate paired samples *T* statistics). To facilitate comparisons of the max(T^2) topographies with the underlying sink-source difference topographies, the sign of the difference at each site was applied to the respective T^2 value, which is otherwise always positive. Please note that symmetric scales optimized for score ranges across new and old stimuli were used for the original topographies. To allow for better comparison of old/new effects across these CSD factors, the same symmetric scale range was used for all difference and max(T^2) topographies, except for the auditory P3 source factor, which showed notably larger old/new effects compared to all other factors. All topographies are two-dimensional representations of spherical spline interpolations ($m = 2$; $\lambda = 0$) derived from the mean factors scores or T^2 statistics available for each recording site.

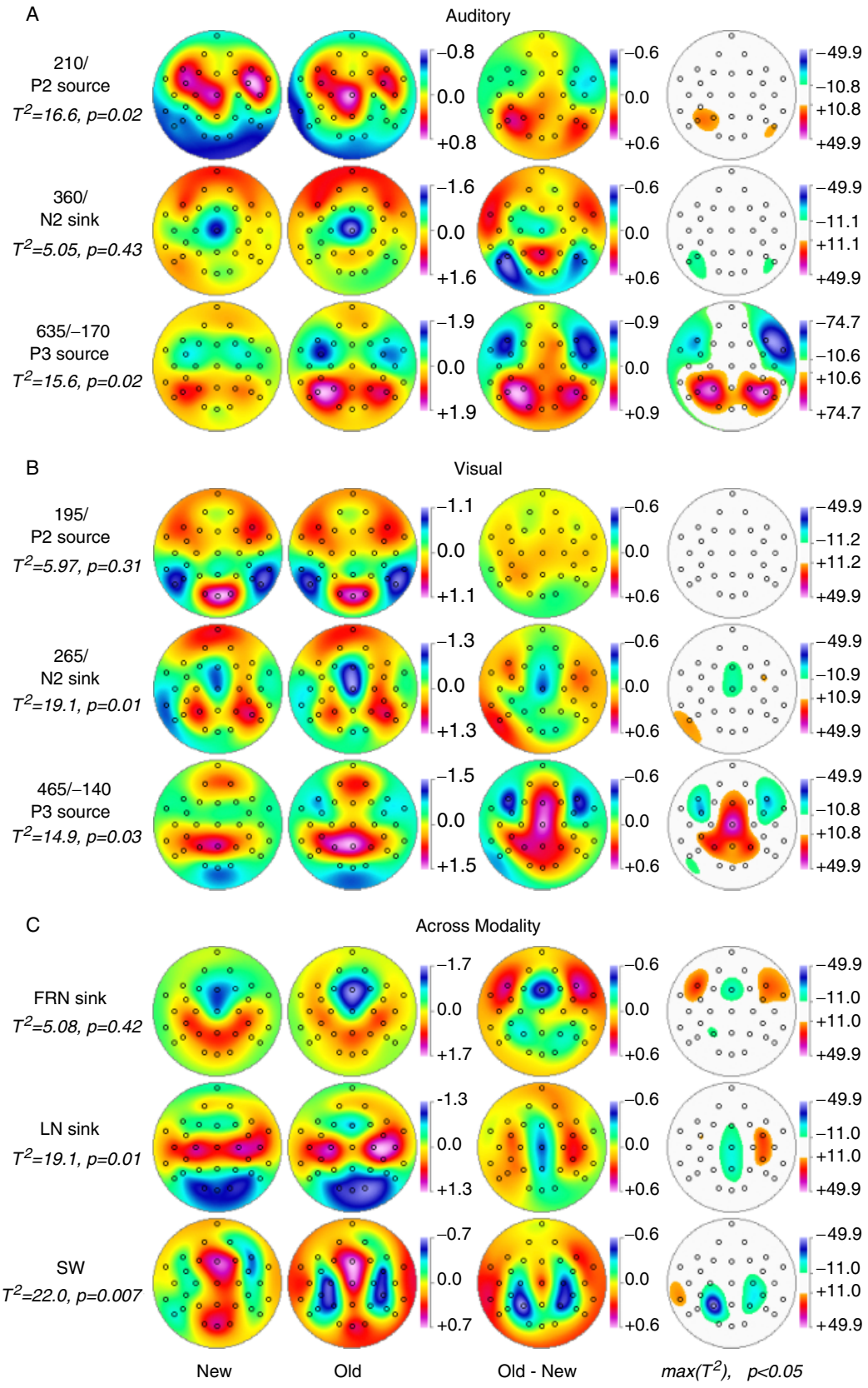
A
Auditory
210/
P2 source
T^2=16.6, p=0.02
−0.8
0.0
+0.8
−0.6
0.0
+0.6
−49.9
−10.8
+10.8
+49.9
360/
N2 sink
T^2=5.05, p=0.43
−1.6
0.0
+1.6
−0.6
0.0
+0.6
−49.9
−11.1
+11.1
+49.9
635/−170
P3 source
T^2=15.6, p=0.02
−1.9
0.0
+1.9
−0.9
0.0
+0.9
−74.7
−10.6
+10.6
+74.7
B
Visual
195/
P2 source
T^2=5.97, p=0.31
−1.1
0.0
+1.1
−0.6
0.0
+0.6
−49.9
−11.2
+11.2
+49.9
265/
N2 sink
T^2=19.1, p=0.01
−1.3
0.0
+1.3
−0.6
0.0
+0.6
−49.9
−10.9
+10.9
+49.9
465/−140
P3 source
T^2=14.9, p=0.03
−1.5
0.0
+1.5
−0.6
0.0
+0.6
−49.9
−10.8
+10.8
+49.9
C
Across Modality
FRN sink
T^2=5.08, p=0.42
−1.7
0.0
+1.7
−0.6
0.0
+0.6
−49.9
−11.0
+11.0
+49.9
LN sink
T^2=19.1, p=0.01
-1.3
0.0
+1.3
−0.6
0.0
+0.6
−49.9
−11.0
+11.0
+49.9
SW
T^2=22.0, p=0.007
−0.7
0.0
+0.7
−0.6
0.0
+0.6
−49.9
−11.0
+11.0
+49.9
New
Old
Old - New
max(T^2), p<0.05

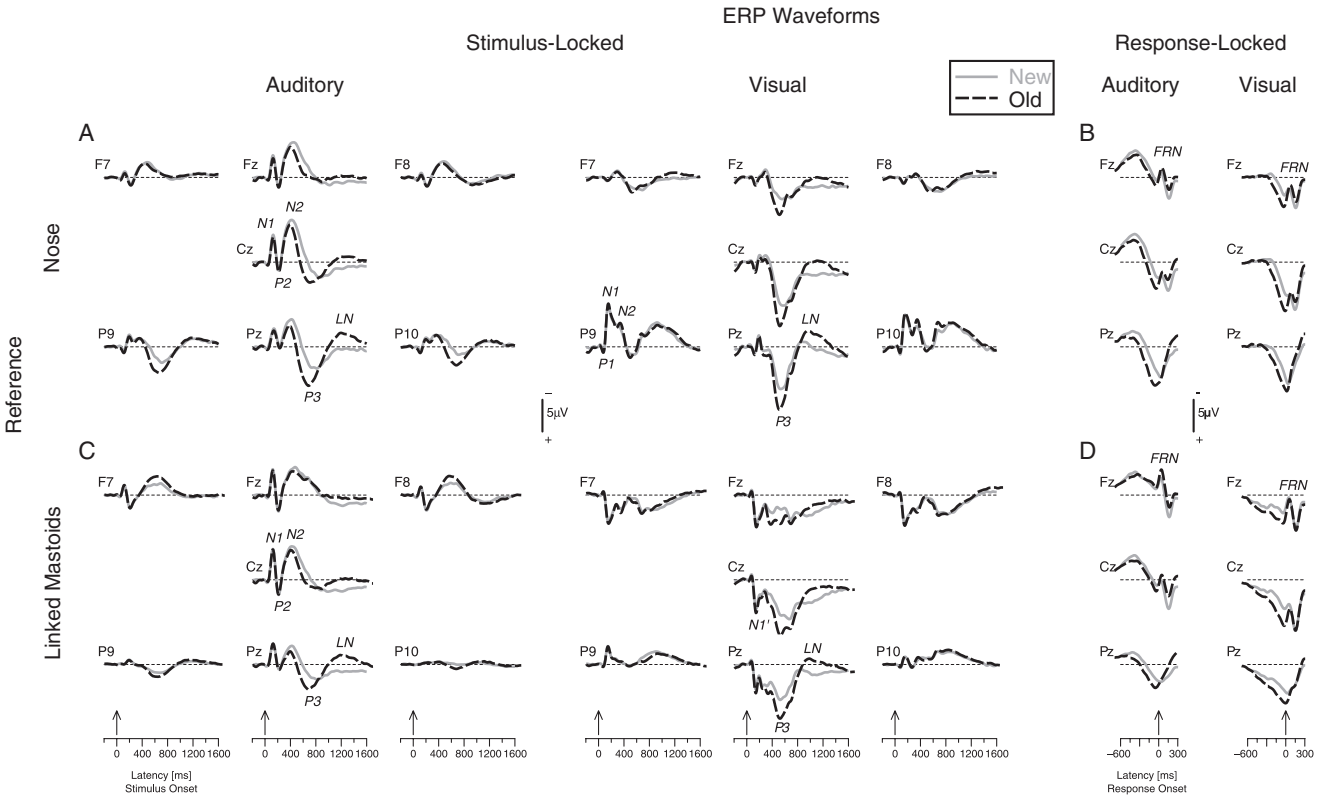

Figure 8. Stimulus-locked (A, C) and response-locked (B, D) grand average ERP waveforms (cf. Figure 1) comparing new and old auditory or visual stimuli at selected sites (Fz, Cz, Pz; F7/8 and P9/10 for stimulus-locked ERPs) using a nose tip (A, B) or linked-mastoids (TP9/10) reference (C, D). All ERPs were baseline corrected to the 100 ms preceding stimulus onset. Due to subtracting the mean mastoid activity, stimulus-locked early negative components (e.g., N1), which are prominent over inferior-lateral sites for visual stimuli when using a nose reference (cf. site P9 in A), are inverted and shifted to midline sites (N1′) when using a linked-mastoids reference (cf. site Cz in C).

PCA is also insensitive in distinguishing temporally coincident sources of variance. It remains to be seen whether these frontal sink-related effects can be dissociated from the parietal source.

In this regard, the visual P3 source factor, with its relatively short latency (465 ms), incorporated a mid-frontal old/new effect, likely related to familiarity (Mecklinger, 2000). However, because it overlapped a mid-frontal source peaking at about 400 ms in the visual CSD waveforms, this contrasts to the mid-frontal negativity (FN400) reported for high-density ERPs using an average reference (Curran, 1999; Curran & Cleary, 2003). Using temporal-spatial PCA, Curran and Dien (2003) reported a dissociation of mid-frontal and parietal old/new effects at about 400 ms poststimulus, but neither their nor this study was designed to separately manipulate familiarity and recognition processes. Recently, however, Curran, DeBuse, Woroch, and Hirshman (2006) showed differential old/new effects after pharmacological intervention with the amnestic drug midazolam, which selectively eliminated the parietal old/new effect and recollection, but did not affect a frontal FN400 old/new effect and presumably familiarity. Whereas Curran and Dien (2003) found no differential FN400 old/new effects to visual test stimuli as a function of study modality (visual, auditory) during a study-test paradigm, concluding that the mid-frontal effect is modality unspecific, our findings lacked a mid-frontal old/new effect at about 400 ms for auditory stimuli, suggesting that the mid-frontal familiarity-related effect can only be probed with visual stimuli. However, an inverted auditory old/new effect was observed at inferior-parietal sites overlapping N2 sink peaking at 360 ms, but it is unclear whether this represents a functional equivalent of an auditory old/new effect related to familiarity. Interestingly, an even earlier positive old/new effect, overlapping the P2 source, was observed for auditory stimuli at almost identical parietal sites. For visual stimuli, an inverted mid-frontocentral old/new effect overlapped N2 sink activity, along with isolated positive old/new effects at sites CP6 and P9. Given the conservative statistical estimates of the randomization tests, these early, modality-specific old/new effects cannot be dismissed; rather, these are likely electrophysiologic correlates of perceptual priming processes (cf. Curran & Dien, 2003). Clearly, more research is needed to understand the impact of processing modality on parietal and frontal old/new effects preceding the subject's response.

Several postresponse old/new effects were highly comparable across modality. Lateral-frontal and inverted mid-frontal old-new effects overlapped a mid-frontal response-related sink (FRN) that followed and terminated the parietal and frontocentral old/new source effects. Although timing (45 ms postresponse) and topography identified the FRN as a prominent postmovement component (N+50; Shibasaki & Hallett, 2006) and likened it to the error-related negativity (ERN/Ne) observed during correct trials (Gehring & Knight, 2000; Vidal, Hasbroucq, Grapperon, & Bonnet, 2000), the overlapping old/new effects strongly suggest ongoing motivational or action-monitoring

processes (e.g., Donkers, Nieuwenhuis, & van Boxtel, 2005; Hajcak, Moser, Holroyd, & Simons, 2006; Luu, Flaisch, & Tucker, 2000). Interestingly, the particular generator pattern of the overlapping old/new effects implied regional dipole activity oriented orthogonally to the cortical surface within the longitudinal fissure (anterior cingulate, supplementary motor area) with opposite orientations in the two hemispheres. This finding is precisely in line with our previous interpretation of focal mid-frontal sink activity observed during target detection tasks, indicating considerable field closure and cancellation at the surface (cf. footnote 4 in Kayser & Tenke, 2006c; Tenke et al., 2007). This descriptive scenario, strongly supported by the CSD evidence, is more consistent with known biophysics of cortical activation than simplified dipole models or other source localization methods representing only open field activity.

The FRN was followed by a late occipital sink reminiscent of the late negativity described previously (e.g., Friedman et al., 2005; Johansson & Mecklinger, 2003; Kayser et al., 2003). It was complemented by a medial centrotemporal source within 100 to 300 ms after response onset, thereby incorporating additional postmovement components (P+50, P+160; Shibasaki & Hallett, 2006). If the posterior sink indeed indexes visual cortex activation during retrieval (Friedman et al., 2005), its highly similar topography for both modalities must then be interpreted as a visualization of word content. However, an overlapping inverted old/new (late episodic memory) effect was not observed over occipital sites, but instead over midline sites (Fz, Cz, Pz), accompanied by old/new effects over mostly right medial frontocentroparietal sites. This topography suggests a generator pattern posteriorly along the cingulate sulcus as hypothesized for the FRN-related old/new effect, an interpretation also supported by the animated CSD topographies. A further extension of the inverted old/new effect into off-midline centroparietal sites overlapped late SW activity, most prominent at P3, a site that also revealed a truly remarkable stimulus-locked synchronization of source and sink old/new effects across modalities (cf. Figure 4A). These observations lead to the tentative conclusions that our late episodic memory effects were triggered by the final evaluation or response decision, roughly coinciding with response onset in recognition paradigms equally stressing speed and accuracy, and reflect action- or self-monitoring processes (Johansson & Mecklinger, 2003).

The combination of CSD and PCA methods as a generic ERP strategy, along with the joint analysis of stimulus- and response-locked activity developed here, appears to be a powerful tool in advancing the understanding of cognitive functions. To this end, our findings indicate that parietal and mid-frontal, positive-going ERP old/new effects between 300 and 800 ms are stimulus related (i.e., precede response onset) and originate from parietal source *and* lateral-frontal sink activity, whereas late occipital, negative-going ERP old/new effects are triggered by the response and originate from bilateral sink activity within anterior cingulate and/or supplementary motor area. Despite the novelty of these findings and the general significance of this methodological approach, the current study is limited by the lack of additional experimental manipulations, other than processing modality. It is unfortunate that the manipulation of task difficulty was evidently ineffective in this sample of healthy adults, as indicated by their behavioral performance data. However, there have been numerous published ERP studies of recognition memory, some of which have been explicitly designed to explore more specific hypotheses (e.g., recollection versus familiarity, etc.). It would be highly informative to apply the present approach to reanalyze these existing ERP data sets.

REFERENCES

Allan, K., Wilding, E. L., & Rugg, M. D. (1998). Electrophysiological evidence for dissociable processes contributing to recollection. *Acta Psychologica*, *98*, 231–252.

Babiloni, F., Cincotti, F., Bianchi, L., Pirri, G., del R.Millan, J., Mourino, J., et al. (2001). Recognition of imagined hand movements with low resolution surface Laplacian and linear classifiers. *Medical Engineering and Physics*, *23*, 323–328.

Chapman, R. M., & McCrary, J. W. (1995). EP component identification and measurement by principal components analysis. *Brain and Cognition*, *27*, 288–310.

Cincotti, F., Babiloni, C., Miniussi, C., Carducci, F., Moretti, D., Salinari, S., et al. (2004). EEG deblurring techniques in a clinical context. *Methods of Information in Medicine*, *43*, 114–117.

Coltheart, M. (1981). The MRC psycholinguistic database. *Quarterly Journal of Experimental Psychology. A, Human Experimental Psychology*, *33*, 497–505.

Curran, T. (1999). The electrophysiology of incidental and intentional retrieval: ERP old/new effects in lexical decision and recognition memory. *Neuropsychologia*, *37*, 771–785.

Curran, T., & Cleary, A. M. (2003). Using ERPs to dissociate recollection from familiarity in picture recognition. *Cognitive Brain Research*, *15*, 191–205.

Curran, T., DeBuse, C., Woroch, B., & Hirshman, E. (2006). Combined pharmacological and electrophysiological dissociation of familiarity and recollection. *Journal of Neuroscience*, *26*, 1979–1985.

Curran, T., & Dien, J. (2003). Differentiating amodal familiarity from modality-specific memory processes: An ERP study. *Psychophysiology*, *40*, 979–988.

Cycowicz, Y. M., Friedman, D., & Snodgrass, J. G. (2001). Remembering the color of objects: An ERP investigation of source memory. *Cerebral Cortex*, *11*, 322–334.

Dien, J. (1998). Issues in the application of the average reference: Review, critiques, and recommendations. *Behavior Research Methods, Instruments, & Computers*, *30*, 34–43.

Dixon, W. J. (Ed.) (1992). *BMDP statistical software manual: To accompany the 7.0 software release*. Berkeley, CA: University of California Press.

Donchin, E. (1966). A multivariate approach to the analysis of average evoked potentials. *IEEE Transactions on Biomedical Engineering*, *13*, 131–139.

Donchin, E., Callaway, R., Cooper, R., Desmedt, J. E., Goff, W. R., Hillyard, S. A., et al. (1977). Publication criteria for studies of evoked potentials (EP) in man. In J. E. Desmedt (Ed.), *Progress in clinical neurophysiology: Vol. 1. Attention, voluntary contraction and event-related cerebral potentials* (pp. 1–11). Basel: Karger.

Donchin, E., & Heffley, E. F. (1978). Multivariate analysis of event-related potential data: A tutorial review. In D.A. Otto (Ed.), *Multidisciplinary perspectives in event-related brain potential research. Proceedings of the Fourth International Congress on Event-Related Slow Potentials of the Brain (EPIC IV)*, Hendersonville, NC, April 4–10, 1976 (pp. 555–572). Washington, DC: The Office.

Donchin, E., Ritter, W., & McCallum, W. C. (1978). Cognitive psychophysiology: The endogenous components of the ERP. In E. Callaway, P. Tueting, & S. H. Koslow (Eds.), *Event-related brain potentials in man* (pp. 349–411). New York: Academic Press.

Donkers, F. C., Nieuwenhuis, S., & van Boxtel, G. J. (2005). Mediofrontal negativities in the absence of responding. *Cognitive Brain Research*, *25*, 777–787.

Fabiani, M., Gratton, G., & Coles, M. G. H. (2000). Event-related brain potentials: Methods, theory, and applications. In J. T. Cacioppo, L. G. Tassinary, & G. G. Bernston (Eds.), *Handbook of psychophysiol-*

ogy (2nd ed, pp. 53–84). Cambridge, UK: Cambridge University Press.

First, M. B., Spitzer, R. L., Gibbon, M., & Williams, J. B. W. (1996). *Structured Clinical Interview for DSM-IV Axis-I Disorders—Non-patient Edition (SCID-NP)*. New York: Biometrics Research Department, New York State Psychiatric Institute.

Friedman, D. (1990a). Cognitive event-related potential components during continuous recognition memory for pictures. *Psychophysiology*, *27*, 136–148.

Friedman, D. (1990b). ERPs during continuous recognition memory for words. *Biological Psychology*, *30*, 61–87.

Friedman, D. (2000). Event-related brain potential investigations of memory and aging. *Biological Psychology*, *54*, 175–206.

Friedman, D., Cycowicz, Y. M., & Bersick, M. (2005). The late negative episodic memory effect: The effect of recapitulating study details at test. *Cognitive Brain Research*, *23*, 185–198.

Friedman, D., & Johnson, R. Jr. (2000). Event-related potential (ERP) studies of memory encoding and retrieval: A selective review. *Microscopy Research and Technique*, *51*, 6–28.

Gehring, W. J., & Knight, R. T. (2000). Prefrontal-cingulate interactions in action monitoring. *Nature Neuroscience*, *3*, 516–520.

Glaser, E. M., & Ruchkin, D. S. (1976). *Principles of neurobiological signal analysis*. New York: Academic Press.

Guillem, F., Bicu, M., Bloom, D., Wolf, M. A., Desautels, R., Lalinec, M., et al. (2001). Neuropsychological impairments in the syndromes of schizophrenia: A comparison between different dimensional models. *Brain and Cognition*, *46*, 153–159.

Hajcak, G., Moser, J. S., Holroyd, C. B., & Simons, R. F. (2006). The feedback-related negativity reflects the binary evaluation of good versus bad outcomes. *Biological Psychology*, *71*, 148–154.

Herron, J. E., Quayle, A. H., & Rugg, M. D. (2003). Probability effects on event-related potential correlates of recognition memory. *Cognitive Brain Research*, *16*, 66–73.

Iidaka, T., Matsumoto, A., Nogawa, J., Yamamoto, Y., & Sadato, N. (2006). Frontoparietal network involved in successful retrieval from episodic memory. Spatial and temporal analyses using fMRI and ERP. *Cerebral Cortex*, *16*, 1349–1360.

Johansson, M., & Mecklinger, A. (2003). The late posterior negativity in ERP studies of episodic memory: Action monitoring and retrieval of attribute conjunctions. *Biological Psychology*, *64*, 91–117.

Johnson, R., Jr. (1995). Event-related potential insights into the neurobiology of memory systems. In F. Boller & J. Grafman (Eds.), *Handbook of neuropsychology, Vol. 10* (pp. 135–163). Amsterdam: Elsevier.

Junghöfer, M., Elbert, T., Tucker, D. M., & Braun, C. (1999). The polar average reference effect: A bias in estimating the head surface integral in EEG recording. *Clinical Neurophysiology*, *110*, 1149–1155.

Kayser, J., Bruder, G. E., Friedman, D., Tenke, C. E., Amador, X. F., Clark, S. C., et al. (1999). Brain event-related potentials (ERPs) in schizophrenia during a word recognition memory task. *International Journal of Psychophysiology*, *34*, 249–265.

Kayser, J., Fong, R., Tenke, C. E., & Bruder, G. E. (2003). Event-related brain potentials during auditory and visual word recognition memory tasks. *Cognitive Brain Research*, *16*, 11–25.

Kayser, J., & Tenke, C. E. (2003). Optimizing PCA methodology for ERP component identification and measurement: Theoretical rationale and empirical evaluation. *Clinical Neurophysiology*, *114*, 2307–2325.

Kayser, J., & Tenke, C. E. (2005). Trusting in or breaking with convention: Towards a renaissance of principal components analysis in electrophysiology. *Clinical Neurophysiology*, *116*, 1747–1753.

Kayser, J., & Tenke, C. E. (2006a). Consensus on PCA for ERP data, and sensibility of unrestricted solutions. *Clinical Neurophysiology*, *117*, 703–707.

Kayser, J., & Tenke, C. E. (2006b). Electrical distance as a reference-free measure for identifying artifacts in multichannel electroencephalogram (EEG) recordings. *Psychophysiology*, *43*, S51.

Kayser, J., & Tenke, C. E. (2006c). Principal components analysis of Laplacian waveforms as a generic method for identifying ERP generator patterns: I. Evaluation with auditory oddball tasks. *Clinical Neurophysiology*, *117*, 348–368.

Kayser, J., & Tenke, C. E. (2006d). Principal components analysis of Laplacian waveforms as a generic method for identifying ERP generator patterns: II. Adequacy of low-density estimates. *Clinical Neurophysiology*, *117*, 369–380.

Kayser, J., Tenke, C. E., Gates, N. A., Kroppmann, C. J., Gil, R. B., & Bruder, G. E. (2006). ERP/CSD indices of impaired verbal working memory subprocesses in schizophrenia. *Psychophysiology*, *43*, 237–252.

Keselman, H. J. (1998). Testing treatment effects in repeated measures designs: An update for psychophysiological researchers. *Psychophysiology*, *35*, 470–478.

Kucera, N., & Francis, W. N. (1967). *Computational analysis of present-day American English*. Providence, RI: Brown University Press.

Lehmann, D. (1984). EEG assessment of brain activity: Spatial aspects, segmentation and imaging. *International Journal of Psychophysiology*, *1*, 267–276.

Lucent Technologies. (2001). Bell labs text-to-speech synthesis. Murray Hill, NJ: Author. Available at: http://www.bell-labs.com/project/tts/voices.html

Luu, P., Flaisch, T., & Tucker, D. M. (2000). Medial frontal cortex in action monitoring. *Journal of Neuroscience*, *20*, 464–469.

Maris, E. (2004). Randomization tests for ERP topographies and whole spatiotemporal data matrices. *Psychophysiology*, *41*, 142–151.

Mecklinger, A. (2000). Interfacing mind and brain: A neurocognitive model of recognition memory. *Psychophysiology*, *37*, 565–582.

Michel, C. M., Murray, M. M., Lantz, G., Gonzalez, S., Spinelli, L., & Grave de Peralta, R. (2004). EEG source imaging. *Clinical Neurophysiology*, *115*, 2195–2222.

Mitzdorf, U. (1985). Current source-density method and application in cat cerebral cortex: Investigation of evoked potentials and EEG phenomena. *Physiological Review*, *65*, 37–100.

Nessler, D., & Mecklinger, A. (2003). ERP correlates of true and false recognition after different retention delays: Stimulus- and response-related processes. *Psychophysiology*, *40*, 146–159.

NeuroScan, Inc. (2003). SCAN 4.3—Vol. II. EDIT 4.3—Offline analysis of acquired data. Document number 2203, Revision D. El Paso, TX: Compumedics Neuroscan.

Nicholson, C. (1973). Theoretical analysis of field potentials in anisotropic ensembles of neuronal elements. *IEEE Transactions on Biomedical Engineering*, *20*, 278–288.

Nunez, P. (1981). *Electric fields of the brain*. New York: Oxford University Press.

Nunez, P. L., & Srinivasan, R. (2006). *Electric fields of the brain: The neurophysics of EEG*. New York: Oxford University Press.

Nunez, P. L., & Westdorp, A. F. (1994). The surface Laplacian, high resolution EEG and controversies. *Brain Topography*, *6*, 221–226.

Oldfield, R. C. (1971). The assessment and analysis of handedness: The Edinburgh inventory. *Neuropsychologia*, *9*, 97–113.

Paivio, A., Yuille, J. C., & Madigan, S. A. (1968). Concreteness, imagery, and meaningfulness values for 925 nouns. *Journal of Experimental Psychology*, *76*, 1–25.

Paller, K. A., & Kutas, M. (1992). Brain potentials during memory retrieval provide neurophysiological support for the distinction between conscious recollection and priming. *Journal of Cognitive Neuroscience*, *4*, 375–391.

Pascual-Marqui, R. D., & Lehmann, D. (1993). Topographic maps, source localization inference, and the reference electrode: Comments on a paper by Desmedt et al. *Electroencephalography and Clinical Neurophysiology*, *88*, 532–536.

Perrin, F., Pernier, J., Bertrand, O., & Echallier, J. F. (1989). Spherical splines for scalp potential and current density mapping [Corrigenda EEG 02274, EEG Clin. Neurophysiol, 1990, 76, 565]. *Electroencephalography and Clinical Neurophysiology*, *72*, 184–187.

Picton, T. W., Bentin, S., Berg, P., Donchin, E., Hillyard, S. A., Johnson, R. Jr., et al. (2000). Guidelines for using human event-related potentials to study cognition: Recording standards and publication criteria. *Psychophysiology*, *37*, 127–152.

Pivik, R. T., Broughton, R. J., Coppola, R., Davidson, R. J., Fox, N., & Nuwer, M. R. (1993). Guidelines for the recording and quantitative analysis of electroencephalographic activity in research contexts. *Psychophysiology*, *30*, 547–558.

Rugg, M. D. (1985). The effects of semantic priming and work repetition on event-related potentials. *Psychophysiology*, *22*, 642–647.

Rugg, M. D. (1987). Dissociation of semantic priming, word and non-word repetition effects by event-related potentials. *Quarterly Journal of Experimental Psychology. A, Human Experimental Psychology*, *39*, 123–148.

Senkfor, A. J., & Van Petten, C. (1998). Who said what? An event-related potential investigation of source and item memory. *Journal of*

Experimental Psychology: Learning, Memory, and Cognition, *24*, 1005–1025.

Shibasaki, H., & Hallett, M. (2006). What is the Bereitschaftspotential? *Clinical Neurophysiology*, *117*, 2341–2356.

Snodgrass, J. G., & Corwin, J. (1988). Pragmatics of measuring recognition memory: Applications to dementia and amnesia. *Journal of Experimental Psychology: General*, *117*, 34–50.

Tenke, C. E., & Kayser, J. (2001). A convenient method for detecting electrolyte bridges in multichannel electroencephalogram and event-related potential recordings. *Clinical Neurophysiology*, *112*, 545–550.

Tenke, C. E., & Kayser, J. (2005). Reference-free quantification of EEG spectra: Combining current source density (CSD) and frequency principal components analysis (fPCA). *Clinical Neurophysiology*, *116*, 2826–2846.

Tenke, C. E., Kayser, J., Fong, R., Leite, P., Towey, J. P., & Bruder, G. E. (1998). Response- and stimulus-related ERP asymmetries in a tonal oddball task: A Laplacian analysis. *Brain Topography*, *10*, 201–210.

Tenke, C. E., Kayser, J., Shankman, S. A., Griggs, C. B., Leite, P., Stewart, J. W., et al. (2007). Hemispatial PCA dissociates temporal from parietal ERP generator patterns: CSD components in healthy adults and depressed patients during a dichotic oddball task. Manuscript submitted for publication.

Urbach, T. P., & Kutas, M. (2006). Interpreting event-related brain potential (ERP) distributions: Implications of baseline potentials and variability with application to amplitude normalization by vector scaling. *Biological Psychology*, *72*, 333–343.

van Boxtel, G. J. M. (1998). Computational and statistical methods for analyzing event-related potential data. *Behavior Research Methods, Instruments, & Computers*, *30*, 87–102.

Vidal, F., Hasbroucq, T., Grapperon, J., & Bonnet, M. (2000). Is the 'error negativity' specific to errors? *Biological Psychology*, *51*, 109–128.

Wagner, A. D., Shannon, B. J., Kahn, I., & Buckner, R. L. (2005). Parietal lobe contributions to episodic memory retrieval. *Trends in Cognitive Sciences*, *9*, 445–453.

Wilding, E. L. (2000). In what way does the parietal ERP old/new effect index recollection? *International Journal of Psychophysiology*, *35*, 81–87.

Wilding, E. L., Doyle, M. C., & Rugg, M. D. (1995). Recognition memory with and without retrieval of context: An event-related potential study. *Neuropsychologia*, *33*, 743–767.

Wilding, E. L., & Rugg, M. D. (1996). An event-related potential study of recognition memory with and without retrieval of source. *Brain*, *119*, 889–905.

Wilding, E. L., & Rugg, M. D. (1997). Event-related potentials and the recognition memory exclusion task. *Neuropsychologia*, *35*, 119–128.

Woodruff, C. C., Hayama, H. R., & Rugg, M. D. (2006). Electrophysiological dissociation of the neural correlates of recollection and familiarity. *Brain Research*, *1100*, 125–135.

Yonelinas, A. P. (2001). Components of episodic memory: The contribution of recollection and familiarity. *Philosophical Transactions of the Royal Society of London. Series B, Biological Sciences*, *356*, 1363–1374.

(Received March 2, 2007; Accepted May 24, 2007)